AFMR 1940
American Federation for Medical Research

https://afmr.org/Western/

Western Society for Pediatric Research

https://www.westernspr.org/

2026 Western Medical Research Conference

(Carmel Meeting)

Total COMP students:

100 with 64 first authors

76 students from Pomona and 24 students from Lebanon

Total COMP abstracts:

65 with 42 oral presentations and 23 poster presentations

51 abstracts from Pomona and 14 abstracts from Lebanon

Madison Dulkanchainun DO2028

won the AFMR Subspecialty Award for Dermatology

Harshini Selvakumar DO2028

won the AFMR Subspecialty Award for Endocrinology & Metabolism.

First Authors

FN	LN	Class
Andrew	Abou Jaoude	DO2028
Erich	Araujo	DONW2028
Lexis	Bates	DONW2026
Isabelle	Bauman	DO2027
Anik	Boyadzhyan	DO2027
Emily	Chen (Han)	DO2027
Erica	Chow	DO2026
Erica	Chow	DO2026
Timothy	Chu	DO2028
Daniel	Damron	DONW2027
Madison	Dulkanchainun	DO2028
Tony	Eskandar	DO2027
Blake	Fardanesh	DO2028
Ethan	Fulsher	DONW2027
Anna	Garrison	DONW2027
Joselyn	Gonzalez	DO2027
Vivek	Gujrathi	DO2027
Vedi	Hatamian	DO2028
Vy	Ho	DO2028
Yeonjoo	Hwang	DONW2028
Shady (Shahdi)	Ibrahim	DO2028
Christopher	Karma	DO2028
Pauneez	Kasmai	DO2028
Chang Kon (Peter)	Kim	DO2028
Jhennis Megan	Lacsamana	DO2026
Kelly	Lam	DO2028
Chantelle	LaNguyen	DO2029
Madeleine	Lu	DO2028
Daniel	Mashiach	DO2027
Joshua	McCluskey	DONW2026
Megan	McKerahan	DO2028
Kristen	Mittl	DONW2028
Samiha	Molla	DO2028

FN	LN	Class
Sukhjinder	Momi	DO2028
Shaanali	Mukadam	DO2028
Niayesh (Nash)	Najafi	DO2028
Ananya	Narasimhan	DO2026
Kenny	Ngo	DO2028
Krystle Jocelyn	Parnala	DONW2027
Jaylan	Patel	DO2028
Hina	Patel	DO2028
Angelie	Pathak	DO2028
Lekha	Pillarisetti	DO2028
Melika	Pirodan	DONW2027
SeyedehParmis (Parmis)	Rejali	DO2028
Edgmin	Rostomian	DO2028
Kimberly	Salazar	DO2028
Nicolaus	Salm	DONW2027
Harshini	Selvakumar	DO2028
Nikita	Shah	DO2027
Eashan	Sharma	DO2028
Akhila	Swarna	DO2028
Caitlin	Tong	DO2027
Isabelle	Tran	DO2028
Tommy	Tran	DO2028
Christina	Trinh	DO2027
Rebecca	Van Dyke	DO2028
Kevin Babakhan	Vartanian	DO2028
Daniel	Vayser	DO2028
Katelyn	West	DONW2027
Chiana	Yang	DO2027
Joseph	Yankee	DONW2027
Vivian	Yu	DO2028
Saher	Zaidi	DONW2027
Amira	Zayed	DO2028

Other Authors

FN	LN	Class
Ryan	Afrahim	DO2027
Arbab	Alam	DO2028
Rasha	Alnajjar	DO2027
Jacqueline	Anderson Enni	DO2028
Luke	Arsenault	DONW2026
Mehr	Boparai	DONW2027
Elizabeth	Chen	DO2027
Lindsey	Chheng	DO2028
Tanzila	Chowdhury	DO2026
Geneva Therese	Dela Cruz	DONW2028
Ishani	Deshpande	DO2026
Amanda	Felty	DONW2027
Jeffrey	Garcia	DONW2028
Zachary	Hall	DO2027
Blake	Han	DO2026
Ryan	Hess	DONW2028
Gursavan	Khatkar	DO2027
Andrea	Leonor	DO2028
Emily	Lyon	DO2027

FN	LN	Class
Peri	McClaskey	DONW2026
Shreyas	Melanahalli	DO2028
Jesse	Melendez	DO2029
Malaika	Menon	DO2028
Colleen	Mercado	DONW2027
Sahana	Natarajan	DONW2029
Brandon	Noorvash	DO2027
Jaylan	Patel	DO2028
Angelie	Pathak	DO2028
Alexander	Postajian	DO2028
Yasmeen	Rabiei	DO2027
Kayvan	Sasaninia	DO2028
Mitchell	Stoddard	DO2027
Shreya	Tamatam	DO2026
Katlin	Wieselthier	DO2026
Alston	Wong	DO2027
Alison	Wyckoff	DONW2027
Sabrina	Yip	DO2026

ORAL PRESENTATIONS

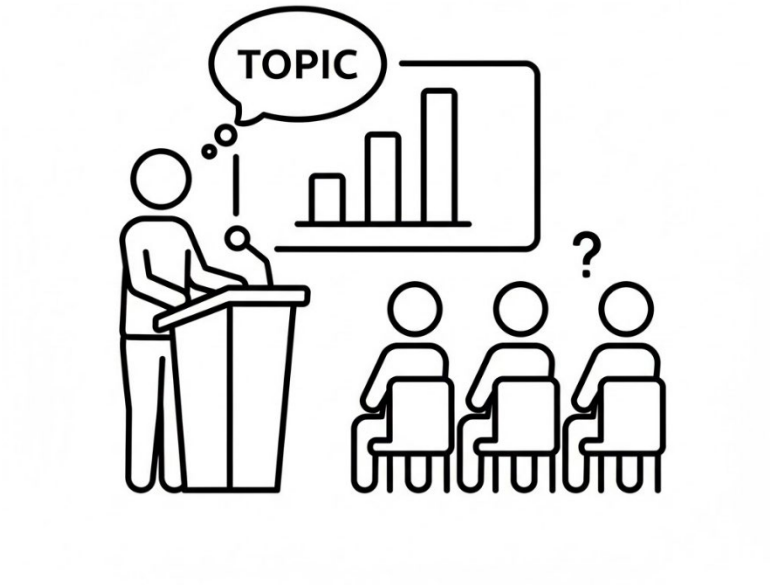

EMERGING PSYCHOSIS WITH AI-FOCUSED DELUSIONS: CASE STUDY OF DIAGNOSTIC COMPLEXITY IN A YOUNG ADULT

C. Trinh[1], E. Gao[2], M. Shenava[2].

[1]Western University of Health Sciences, Pomona, California, UNITED STATES|

[2]Kaiser Permanente Bernard J Tyson School of Medicine, Pasadena, California, UNITED STATES|

ABSTRACT BODY:

Case Report: In this case study, we examine the diagnostic and therapeutic challenges posed by a 19-year-old male with a psychiatric history of ADHD, generalized anxiety disorder, and Tourette's, who presented with emerging psychosis. Notably, he had no prior psychiatric hospitalizations but had been using cannabis wax pens regularly for several months. Collateral history revealed progressive decompensation characterized by escalating paranoia, social withdrawal, minimal oral intake, severe sleep deprivation, a 20-pound weight loss, and intermittent suicidal thoughts. On presentation, the patient demonstrated labile affect, pressured and tangential speech, and overt cheerfulness despite clear disorganization. He denied hallucinations but described "classified" intrusive thoughts and a unique capacity to detect "patterns and parallels" imperceptible to others. His delusional system was heavily AI-focused, including beliefs that artificial intelligence (AI) was responsible for COVID-19 and that his social isolation stemmed from "misaligned beliefs about AI." He personified AI as "Athena" and frequently referenced concepts such as ego death and the heat death of the universe. His psychiatric history also included episodes of self-harm through scratching and repeated needle puncturing of his foot, as well as an emotional breakdown after peers rejected his AI-related proposals in student council.

During hospitalization, treatment with olanzapine and valproic acid led to gradual mood stabilization and decreased behavioral disorganization, though AI-themed delusional beliefs persisted. The diagnostic picture remained complex, with considerations including primary psychosis, bipolar spectrum illness, ADHD and Tourette's-related features, and cannabis use as an exacerbating factor.

This case underscores the evolving role of cultural and technological content in shaping delusional themes. Emerging patterns include spiritual awakenings centered on AI, perceptions of AI as sentient, and attachment-based delusions in which chatbot interactions are misinterpreted as genuine emotional reciprocity. Such presentations raise unique diagnostic challenges, as clinicians must distinguish between psychosis, substance-induced exacerbation, and culturally mediated speech. Cross-referencing chatbot outputs may provide a novel strategy to clarify whether AI-related content reflects true delusional thinking or external influences thereby guiding more accurate diagnosis and treatment.

INCREASING TRENDS IN CONSCIENTIOUS EXEMPTION RATES FOR CHILDHOOD VACCINATIONS IN TWO ADJACENT WEST TEXAS COUNTIES AMIDST THE 2025 MEASLES OUTBREAK

N. Shah[1], M.G. Stoddard[1], A. Pumerantz[1], Y. Shono[2].

[1]Western University of Health Sciences College of Osteopathic Medicine of the Pacific, Pomona, California, UNITED STATES|

[2]School of Community and Global Health, Claremont Graduate University, Claremont, California, UNITED STATES|

ABSTRACT BODY:

Purpose of Study: As of August 12, Texas has reported 762 measles cases year-to-date for 2025. In west Texas, Gaines County reported 414 cases, while adjacent Andrews County reported only three. Conscientious exemptions (non-medical exemptions, NMEs) from childhood immunizations are often related to parental vaccine hesitancy, which threaten herd immunity contributing to measles outbreaks. We previously obtained vaccine exemption data among kindergartners from Centers for Disease Control and Prevention (CDC) and Texas Department of State Health Services (DSHS) to analyze NME trends at the national and Texas county-levels between 2013 and 2024. We found that mean NME rates in Gaines were 12-fold higher than in Andrews. Here, we continued our trend analysis to include 2024-2025.

Methods Used: National kindergarten immunization exemption data from 2011–2025 were obtained from CDC. Medical exemption rates were excluded due to stability. Texas county-level NME data from 2013–2025 were obtained from DSHS. Of 254 Texas counties, Andrews matched closest to Gaines in population size and demographics. LOESS curves, Spearman correlations with calendar year, and Welch's t-tests assessed inter-county trend differences. Analyses were performed in SPSS v30 with significance set at $p<0.05$.

Summary of Results: Between 2024 and 2025, NME rates increased from 17.62% to 19.49% in Gaines County and from 1.99% to 4.53% in Andrews County. Calendar year was strongly associated with NMEs nationally ($\rho = 0.742$, $p = 0.006$) and in Gaines ($\rho = 0.741$, $p = 0.006$), while there was a weaker, non-significant association in Andrews ($\rho = 0.357$, $p = 0.255$). Welch's t-test showed a significant difference between Gaines (mean = 15.22, SD = 4.34) and Andrews (mean = 1.49, SD = 1.23), $t(12.76) = 10.55$, $p < 0.001$. The difference in means was 13.73 (95% CI: 10.91–16.55) with a very large effect size (Hedges' $g = 4.16$, 95% CI: 2.59–5.73). LOESS curves and Spearman rankorder correlations were consistent.

Conclusions: Conscientious exemption rates in Gaines County continue to rise amidst the ongoing Texas measles outbreak. While in adjacent Andrews County a marked spike in NME rates over the past year raises concerns about inter-county spillover of vaccine hesitancy that may further threaten herd immunity. With continued vigilance, the trajectory of rising exemptions may still be redirected toward improved vaccination coverage.

LONGITUDINAL TRANSCRIPTOMIC SIGNATURES OF PERSISTENT POST-TRAUMATIC HEADACHE AFTER MILD TRAUMATIC BRAIN INJURY

T. Nguyen[1], T. Hato[1], K.M. Naugle[1], F. White[1], I.T. Tran[2].

[1]Indiana University School of Medicine, Indianapolis, Indiana, UNITED STATES|

[2]Western University of Health Sciences, Pomona, California, UNITED STATES|

ABSTRACT BODY:

Purpose of Study: Post-traumatic headache (PTH) is a prevalent, yet poorly understood, complication of mildtraumatic brain injury (mTBI). While past transcriptomic studies have described acute and cross-sectional changes following mTBI, this study aims to identify longitudinal signatures distinguishing PTH at subacute and chronic timepoints.

Methods Used: This pilot study compared 12 adults with persistent PTH after mTBI and 10 age- and sex-matched healthy controls. Peripheral blood mononuclear cells were collected at 3 (subacute) and 6 (chronic) months post injury. RNAseq data were analyzed in R (V4.3.0) with edgeR/limma. Principal component analysis revealed strong sex-driven variation. Pathway enrichment was conducted using Enrichr across KEGG, Reactome, and WikiPathways databases. Composite Feature Evaluation (CFE) integrated gene expression, pathway enrichment, STRING connectivity, and literature evidence to prioritize candidate biomarkers.

Summary of Results: CFE scoring highlighted Vav Guanine Nucleotide Exchange Factor 3 (VAV3) and Small Nuclear Ribonucleoprotein U1 Subunit 70 (SNRNP70) as top candidate biomarkers. VAV3's role in immune migration and nerve repair, suggests a part in PTH duration. SNRNP70 links RNA splicing deficits to chronic pain. Other gene candidates include Potassium 2 Pore Domain Channel Subfamily K Member 6 (KCNK6), which may enhance neuronal hyperexcitability and disrupt inflammasome control, and Phosphoinositide-3-Kinase Adaptor Protein1 (PIK3AP1,) which is linked to toll-like receptor signaling and injury response. ADP Ribosylation Factor Like GTPase6 Interacting Protein 4 (ARL6IP4), which exhibited bidirectional regulation across timepoints, is consistent with stress response adaptation. Enrichment analyses converged on Rho GTPase signaling, phagocytosis pathways, and immune receptor signaling. These results suggest immune receptor signaling, cytoskeletal remodeling, and RNA splicing as key biological processes in chronic PTH.

Conclusions: This study suggests distinct longitudinal shifts in peripheral immune expression distinguishing PTH from recovery. Candidate genes show promise as biomarkers and therapeutic targets. Transcriptomic shifts may hold prognostic value for identifying patients at risk of persistent PTH and a therapeutic window. These findings provide insight into neuroimmune pathophysiology of prolonged PTH and lay the groundwork for larger studies to improve diagnosis and treatment of chronic post-traumatic pain.

PICROSIRIUS RED STAINING AND POLARIZED MICROSCOPY: A POTENTIAL TOOL FOR BURN DEPTH GRADING WITH ENHANCED REPRODUCIBILITY

C. LaNguyen[1], C. LaNguyen[2], N. Wakida[2], C. Campbell[2], G. Kennedy[2], A. Durkin[2].

[1]Western University of Health Sciences, Pomona, California, UNITED STATES|

[2]University of California Irvine Beckman Laser Institute & Medical Clinic, Irvine, California, UNITED STATES|

ABSTRACT BODY:

Purpose of Study: Burn injuries activate immune and inflammatory responses that influence tissue repair. Histological analysis assesses injury progression and healing in preclinical models. Traditional stains like H&E and Masson's Trichrome are widely used, but interpretation can be inconsistent, and distinguishing superficial from deep partial-thickness burns remains difficult due to poorly defined boundaries.

This study explores Picrosirius Red (PSR) staining with polarized light microscopy to visualize and quantify collagen changes in burns. PSR enhances collagen birefringence and, when paired with immunohistochemistry, can differentiate collagen types I and III. We evaluate PSR's utility in identifying collagen denaturation depth across burn severities, especially between superficial and deep partial-thickness burns.

Methods Used: Thermal burns were administered to anesthetized Yorkshire pigs using a brass probe at 100°C (at constant pressure) with contact durations varying from 5 seconds to 40 seconds to achieve burn severities across the entire range from superficial to full thickness. Full-thickness samples were collected at 1, 7, 14, 21, and 28 days postburn, then fixed, sectioned, and PSR-stained. Collagen architecture was imaged under polarized light, and damage depth was quantified using ImageJ. Ratios of damaged to intact collagen were calculated to assess correlations between exposure time and degradation.

Summary of Results: The results reveal that PSR staining effectively captures the dynamic progression of burn tissue healing over time, providing a clear visualization of collagen remodeling across varying burn durations. This allows for a greater understanding of how thermal injury severity influences tissue repair processes, enabling differentiation for partial thickness burn depths based on collagen fiber organization, density, and birefringence.

Conclusions: When combined with immunohistochemistry labeling, we can distinguish between collagen types I and III which can aid in differentiation between bone formation and fibrosis. This method offers potential for standardization in histological evaluation and may serve in developing machine learning models capable of automating burn grading.

CARDIAC REGENERATIVE ROLE OF LGALS1 IN EPICARDIAL ADIPOSE TISSUE STROMAL CELLS

V. Hatamian[1,2], F.G. Thankam[1].

[1]Department of Translational Research, Western University of Health Sciences College of Osteopathic Medicine of the Pacific, Pomona, California, UNITED STATES|

[2]Translational Research, Western University of Health Sciences, Pomona, California, UNITED STATES|

ABSTRACT BODY:

Purpose of Study: Myocardial infarction (MI) leads to irreversible cardiomyocyte (CM) loss, fibrotic scar formation, and progressive heart failure. Epicardial adipose tissue (EAT), a metabolically active fat layer surrounding the heart, directly communicates with the myocardium and modulates post-MI repair through paracrine signaling. We identified that EAT-derived stromal cells (EATDS) secrete Galectin-1 (LGALS1), a cardioprotective protein, under ischemic stress. We hypothesized that LGALS1 drives CM-differentiation of EATDS enhancing cardiac repair. Our objective was to understand the mechanisms underlying LGALS1-driven cardiac protection in EATDS.

Methods Used: EATDS were isolated from the EAT of Yucatan swine and cultured under ischemic conditions. LGALS1 in the EATDS were genetically inhibited using CRISPR/Cas9-mediated global knockout (KO) and silenced by RNA interference (RNAi)-mediated knockdown (KD) to assess the cardioprotective effects. Then, the expression status of CM-specific genes (GATA4, Nkx2.5, CX43, TBX5, IRX4, and cTnI) was evaluated in LGALS1 KO and KD EATDS by PCR, immunofluorescence, and Western blot analysis.

Summary of Results: LGALS1 KO (Log2 FC -7.36 ± 0.48) and KD (Log2 FC -6.33 ± 0.05) EATDS cells were successfully established. Both KO and KD of LGALS1 in EATDS significantly downregulated CM-specific markers compared to controls at both mRNA and protein levels. Notably, the inhibition of LGALS1 in EATDS impaired the expression of transcription factors and structural proteins critical for CM identity and function, indicating its role in promoting differentiation of EATDS toward a CM-like phenotype. Quantitative PCR analysis further demonstrated marked downregulation of cardiac marker expression, with KO cells relative to controls, confirming the robustness of transcriptional suppression.

Conclusions: LGALS1+ EATDS play a crucial role in regulating cardiac repair mechanisms by upregulating CMspecific genes (GATA4, Nkx2.5, CX43, TBX5, IRX4, and cTnI) and survival signaling under ischemic conditions. These findings highlight the translational potential of LGALS1+EATDS for myocardial regeneration following MI.

DOES THE PROSPECTIVE FLOW CYTOMETRY CROSSMATCH PREDICT POST-HEART TRANSPLANT AMR OR OTHER OUTCOMES?

C.P. Kim, M. Lee, P. Deckerman, N. Satish, M. Hamilton, J. Kobashigawa.
Cedars-Sinai Smidt Heart Institute, Los Angeles, California, UNITED STATES|

ABSTRACT BODY:

Purpose of Study: Highly sensitized patients awaiting heart transplantation are at greater risk for the development of hyperacute rejection. In these cases, we mandate a prospective Complement Dependent Cytotoxicity (CDC) crossmatch as well as a flow cytometry crossmatch for these patients. We will only proceed with heart transplantation if the CDC crossmatch is negative despite the level of antibodies detected by flow cytometry, which is characterized as median channel shifts (MCS). It has not been demonstrated whether the degree of MCS correlates to increased risk of antibody mediated rejection after heart transplantation.

Methods Used: Between 2010 and 2023, we assessed 44 heart transplant patients, highly sensitized patients, who had prospective CDC and prospective flow cytometry crossmatch prior to heart transplant. We only included cases where the CDC crossmatch was negative, and a flow cytometry crossmatch was performed. Patients were divided into those with MCS: <125 MCS, 125-200 MCS, 200-300 MCS, and >300 MCS. These 4 groups were then compared for 1-year freedom from acute cellular rejection (ACR≥2R), antibody-mediated rejection (pAMR ≥1), and biopsy-negative rejection (BNR). Other endpoints include 1-year survival, 1-year freedom from cardiac allograft vasculopathy (CAV), left ventricular dysfunction (LVEF ≤40%), and de novo donor-specific antibody (DSA).

Summary of Results: Qualitatively, those patients with a positive prospective flow cytometry crossmatch of greater than 125 MCS had lower freedom from AMR in the first year after heart transplantation. Flow cytometry crossmatch of less than 125 MCS had the greatest freedom from AMR in the first year after transplant. There appeared to be no difference in the study groups for 1-year survival, freedom from 1-year ACR, BNR, CAV, LVD and de novo DSA. Conclusions: Sensitized patients awaiting heart transplantation where the prospective was CDC negative, but positive flow cytometry crossmatch appear to be at risk for more first-year AMR. These patients might be considered for more anti-humoral immunosuppression to prevent the downstream development of AMR. However, larger number of patients are needed to confirm these findings.

INFECTIOUS MICROBIAL SPECIES IN JACKSTONE FORMATION

D. Mashiach[1], R. Alnajjar[1], B. Noorvash[1], R. Afrahim[1], V.H. Canela[2,3], J.C. Williams[3], E. Fricano[1], H. Szurmant[1].

[1]College of Osteopathic Medicine of the Pacific, Western University of Health Sciences, Pomona, California, UNITED STATES|

[2]Butler University, Indianapolis, Indiana, UNITED STATES|

[3]Indiana University School of Medicine, Indianapolis, Indiana, UNITED STATES|

ABSTRACT BODY:

Purpose of Study: Jackstone calculi are rare urinary stones with a distinctive spiculated structure, most often composed of calcium oxalate monohydrate. While microbial associations have been reported in other urinary stones, no microbial analysis has ever been conducted on a jackstone. This study aims to investigate whether infectious microbial species are embedded within bladder jackstones, providing novel insights into their formation and potential pathways for prevention and treatment.

Methods Used: Twenty-four jackstone calculi were collected: one from the bladder of a donor body in the Western University of Health Sciences anatomy laboratory, and 23 from a stone analysis facility (Beck Analytical Services, Greenwood, IN). Microbial sampling was performed by swabbing the external surface of the calculus arms and by crushing the stone body. DNA was extracted and amplified using universal bacterial primers (27F and 1492R) targeting the V1–V8 regions of the 16S rRNA gene. Amplicons underwent Sanger and next-generation sequencing to characterize the microbial community associated with the jackstone.

Summary of Results: Sanger sequencing of DNA derived from the external swab and crushed body samples of the donor body stone demonstrated mixed microbial communities, with Cutibacterium acnes identified as the dominant species in the crushed body. Next-generation sequencing further revealed distinct and diverse microbial communities in both samples. The external arm was dominated by Lactobacillus (35%), Corynebacterium (20%), Achromobacter (20%), and Ralstonia (13%), whereas each of these genera was <1% in the body. In contrast, the stone body was enriched for Staphylococcus (30%), Abiotrophia (15%), Streptococcus (12%), and Cutibacterium (10%), with these genera each <1% of the stone arm. Analyses of the remaining 23 jackstones are in progress.

Conclusions: These findings suggest a stratified microbial community, with distinct taxa on the external surface and unusual species at the stone core, organisms likely present at the time of stone formation and potentially contributing to jackstone seeding. Notably, C. acnes, previously linked to benign prostatic hypertrophy (BPH), was abundant in the donor stone, raising the possibility that BPH-associated urinary stasis facilitated colonization and stone development. Analysis of the remaining 23 jackstones will provide further evidence into the consistency and potential significance of C. acnes or other species in jackstone formation.

A RARE CAUSE OF VERTEBRAL OSTEOMYELITIS CAUSED BY STREPTOCOCCUS SALIVARIUS

S.F. Zaidi[1], R. Johal[2], P.G. McClaskey[3], J. Patel[4], S. Mishra[4].

[1]Western University of Health Sciences College of Osteopathic Medicine of the Pacific-Northwest, Lebanon, Oregon, UNITED STATES|

[2]California Health Sciences University, Clovis, California, UNITED STATES|

[3]Western University of Health Sciences College of Osteopathic Medicine of the Pacific-Northwest, Lebanon, Oregon, UNITED STATES|

[4]Infectious Disease, Kern Medical, Bakersfield, California, UNITED STATES|

ABSTRACT BODY:

Case Report: Vertebral Osteomyelitis (VO) is a rare but serious infection of the spine, most commonly from hematogenous spread. Incidence has increased in recent decades, particularly among older and immunocompromised patients. Staphylococcus aureus remains the predominant pathogen, while oral streptococci, including Streptococcus salivarius, are rare etiologies. Only three cases have been reported, underscoring the novelty of this case. Disruption of the oral mucosa can cause transient bacteremia, with dental procedures a recognized risk. Although uncommon, odontogenic origins may be overlooked without careful evaluation.

A 51-year-old male with history of splenectomy after trauma, cervical epidural abscess due to MRSA treated with decompressive laminectomy and prolonged daptomycin, and eventual recovery of his neurological deficits one year prior, presented with three months of progressive back pain, two months of fatigue, bilateral lower extremity weakness associated with bowel incontinence, and a 10-lb weight loss. He was afebrile, hemodynamically stable, with 3/5 bilateral lower extremity strength. Labs were unremarkable except for mildly elevated BUN, and blood cultures were negative. MRI of Lumbar spine with and without contrast revealed new L5–S1 disc and adjacent endplate edema with mild prevertebral enhancement concerning osteomyelitis versus discitis. Antibiotics were held, and a CT-guided bone biopsy showed positive culture for S. salivarius. The patient was treated with IV ceftriaxone for 6 weeks via PICC, with clinical improvement. Further history revealed dental extractions and denture placement, five months prior to symptom onset, a likely source for infection.

While S. aureus accounts for the majority of vertebral osteomyelitis (VO) cases, S. salivarius should also be considered in patients with a history of dental interventions or oral disease. Rare reports, including the present case, highlight that S. salivarius, although typically an oral commensal, can serve as a nidus for VO following dental manipulation. Our case adds to the growing body of evidence suggesting that oral bacteria may play a larger role in VO than previously assumed. This underscores the importance of incorporating a thorough dental history and oral examination into the evaluation of patients with VO. By broadening the differential to include oral flora, clinicians may improve diagnostic accuracy and guide more tailored management strategies.

THE ROLES OF THE OPIOID SYSTEM IN BINGE EATING AND FOOD DEVALUATION

K. Salazar[1], I. Era[1], H. Nguyen[2], A. Hamid[2], K. Lutfy[2].

[1]College of Osteopathic Medicine of the Pacific, Western University of Health Sciences, Pomona, California, UNITED STATES|

[2]Western University of Health Sciences, Pomona, California, UNITED STATES|

ABSTRACT BODY:

Purpose of Study: The rate of obesity continues to increase at an alarming rate, urging the need to understand the mechanisms modulating palatable food consumption and binge eating, important contributors of obesity. Thus, the purpose of this study is to investigate the role of enkephalin and β-endorphin in regulating binge eating and food devaluation, using single and double knockout mouse models.

Methods Used: Male mice lacking enkephalin (n=8) or β-endorphin (n=9), along with their respective wildtype controls (n=8, n=9 respectively) were used to assess the role of each opioid peptide in binge eating and food devaluation. To further examine potential interactions between the two peptides, mice lacking both enkephalin and β-endorphin (n=8) and their wildtype controls (n=5) were also included in this study. Mice were individually housed to habituate to the new environment for 1 week. Baseline intake of regular chow diet (RCD) was then measured at 24 h. Mice were then given a high-fat diet (HFD) with intake recorded at 1 h and 24 h followed by RCD exposure for 4 weeks before tested for binge eating in which they were given HFD and their 1 h intake was measured and compared to their initial intake of HFD. Mice remained on HFD for 1 week. To measure food devaluation, mice were returned to RCD and intake was recorded at 24 h and compared to their baseline RCD intake. Additionally, the body weight of each mouse was also recorded on each test day.

Summary of Results: All mice exhibited binge eating behavior. However, binge eating was reduced in mice lacking β-endorphin than their wildtype controls ($p \leq 0.05$). Food devaluation remained intact in single knockout mice ($p > 0.05$) but was reduced in enkephalin/β-endorphin double knockout mice compared to their wildtype controls, as double knockout mice showed more RCD intake at devaluation compared to wildtype controls ($p \leq 0.01$). Additionally, body weight was significantly higher in enkephalin/ β-endorphin double knockout mice compared to their respective wildtypes at baseline ($p \leq 0.05$) and at the end of the study ($p \leq 0.01$).

Conclusions: β-endorphin contributes to the regulation of binge eating while both peptides may contribute to food devaluation. Together, these results suggest that β-endorphin is involved in binge eating and body weight regulation but both enkephalin and β-endorphin are needed in regular-diet devaluation.

FIBROSIS AND CARDIAC REMODELING UNDER METABOLIC STRESS: EXPRESSION OF GALECTIN-3, TRANSFORMING GROWTH FACTOR BETA 1, AND BRAIN NATRIURETIC PEPTIDE

H. Patel, A. Pathak, R. Rajalekshmi, D.K. Agrawal.

College of Osteopathic Medicine of the Pacific, Western University of Health Sciences, Pomona, California, UNITED STATES|

ABSTRACT BODY:

Purpose of Study: Adverse cardiac remodeling, driven by chronic metabolic conditions such as hyperlipidemia and hyperglycemia, is a precursor to heart failure. The molecular basis for this process is not yet fully understood. Galectin-3 (Gal-3) is a protein involved in inflammation and fibrosis, transforming growth factor-beta 1 (TGF-β1) promotes fibrous tissue deposition and heart scarring, and elevated brain natriuretic peptide (BNP) may indicate heart failure. Cardiac remodeling and heart failure progression is driven by signaling pathways orchestrated by these mediators. We investigated the effects of metabolic conditions on the expression of Gal-3, TGF-β1, and BNP in the left ventricular (LV) tissue of control (healthy; N=6), hyperlipidemic (HYL; blood cholesterol 450-700 mg/dL; N=6), and hyperglycemic (HYG; blood glucose 100- 300 mg/dL; N=6) Yucatan miniswine.

Methods Used: Fresh LV tissues were isolated and formalin-fixed and paraffin-embedded for histopathology with Hematoxylin & Eosin (H&E) and Trichrome stains. mRNA transcripts of Gal-3, TGF-β1, and BNP were evaluated by qRT-PCR and protein expression was assessed by Western blot and immunohistochemistry (IHC).

Summary of Results: Well-organized myocytes, intact intercalated discs, and minimal interstitial collagen deposition were found in control myocardium. Ventricular tissues of HYL and HYG swine displayed myocyte hypertrophy, extensive interstitial fibrosis, and inflammatory infiltrates. HYL tissue also demonstrated focal fat infiltration. Gene expression was upregulated in both conditions compared to controls: Gal-3 - HYL: 2.42-fold, HYG: 2.30-fold; TGF-β1 - HYL: 1.03-fold, HYG: 1.66-fold; and BNP - HYL: 5.27-fold, HYG: 2.05-fold. There was a positive correlation between transcript and blood glucose levels (Gal-3: R = 0.64; BNP: R = 0.64; TGF-β1: R = 0.51). Western blot analysis confirmed increased Gal-3, BNP, and active TGF-β1 protein levels, but precursor TGF-β1 was reduced in HYL and elevated in HYG samples. IHC staining localized Gal-3 around ventricular vasculature, BNP within Purkinje fibers, and TGF-β1 to the nuclear and perinuclear (Golgi-associated) regions of cardiomyocytes. Elevated expression of all markers was observed in response to metabolic stress compared to normal swine.

Conclusions: The findings highlight the role of Galectin-3 and BNP as measurable biomarkers for the development of heart disease associated with metabolic syndrome and as potential therapeutic targets for intervention.

THE ROLE OF PPARδ IN LIPID DROPLET ACCUMULATION IN MICROGLIA

C. Karma[1], A. La Spada[2].

[1]College of Osteopathic Medicine of the Pacific, Western University of Health Sciences, Pomona, California, UNITED STATES|

[2]Department of Pathology, School of Medicine, University of California Irvine, Irvine, California, UNITED STATES|

ABSTRACT BODY:

Purpose of Study: Peroxisome proliferator-activated receptor delta (PPARδ) is a ligand-activated transcription factor highly expressed in microglia, where it regulates lipid metabolism and anti-inflammatory pathways. Microglia in Alzheimer's disease (AD) often adopt a lipid droplet–accumulating, pro-inflammatory phenotype that contributes to disease pathology. This study aimed to determine whether pharmacologic activation of PPARδ reduces lipid droplet accumulation in microglia, thereby restoring a more physiologic phenotype and supporting its role as a potential therapeutic target in AD and other neurodegenerative diseases.

Methods Used: BV2 murine microglial cells were cultured under standard conditions and treated with either vehicle (DMSO), oleic acid (OA; 20 μM) to induce lipid droplet formation, GW501516 (GW; 500 nM) to agonize PPARδ, or combinations (OA+GW, OA+TrC). Cells were fixed and stained with Hoechst 33342 (nuclear marker) and BODIPY (neutral lipid dye). Confocal microscopy was performed to acquire 10 random z-stack images per well at 20xmagnification, across three independent trials. Mean fluorescence intensity of BODIPY signal per cell area was quantified and normalized to controls. PPARδ target engagement was confirmed by qRT-PCR for ANGPTL4 and UCP2, normalized to GAPDH. Statistical analysis was performed using a nested one-way ANOVA.

Summary of Results: GW treatment significantly upregulated ANGPTL4 and UCP2 expression, validating effective PPARδ agonism. OA robustly induced lipid droplet accumulation compared to controls ($p < 0.001$). Co-treatment with GW significantly decreased lipid accumulation compared to OA alone ($p < 0.01$) and to a degree comparable to triacsin C, a known inhibitor of triacylglycerol synthesis. No significant differences were observed between control and GW-only groups, indicating that PPARδ activation primarily impacts lipid accumulation under stimulated, not basal, conditions.

Conclusions: PPARδ agonism with GW501516 effectively reduces OA-induced lipid droplet accumulation in microglial cells, supporting a regulatory role for PPARδ in microglial lipid metabolism. These results suggest that pharmacologic activation of PPARδ could mitigate the pro-inflammatory, lipid-laden microglial phenotype observed in AD and represents a promising therapeutic avenue. Future studies should validate these findings in APOE4 or human iPSCderived microglial models and examine additional lipid droplet characteristics such as size, number, and density to further clarify PPARδ's functional impact.

NORMOTHERMIC EX VIVO PERFUSION WITH HEPARINIZED AUTOLOGOUS BLOOD EXTENDS FREE FLAP VIABILITY BEYOND COLD STORAGE

N. Najafi[1], A. Meyers[2], D. Phuyal[2], A. Rampazzo[2], B. Bassiri Gharb[2].

[1]Western University of Health Sciences, Pomona, California, UNITED STATES|

[2]Plastic Surgery, Cleveland Clinic, Cleveland, Ohio, UNITED STATES|

ABSTRACT BODY:

Purpose of Study: The aim of this study was to evaluate an autologous blood-based ex vivo perfusion (EVP) protocol for vascularized composite tissue preservation. Building upon prior HBOC-201 based models, we hypothesized that EVP with heparinized porcine blood and optimized gas composition could sustain free flaps under near-physiologic conditions for 24 h, exceeding the viability of standard cold storage (SCS).

Methods Used: Ten Yorkshire pigs provided bilateral abdominal fasciocutaneous flaps based on superior epigastric perforators (n=20). One flap per animal was perfused for 12 h (n=5) or 24 h (n=5) using a custom EVP circuit primed with HBOC-201 and human albumin; contralateral flaps served as SCS controls at 4°C (n=10). Monitored parameters included hemodynamics, perfusate gases, metabolites, electrolytes, and flap weight. Indocyanine green angiography and infrared thermography assessed microvascular perfusion, while biopsies every 6 h underwent histology and caspase-3 immunohistochemistry.

Summary of Results: Warm ischemia time averaged 16 ± 6 min. Hemodynamics, pH, oxygenation, electrolytes, and metabolic markers were comparable between 12 h and 24 h EVP groups at perfusion end. Flap weight remained stable in both groups (12 h +1.2% [–1.1% to +1.6%]; 24 h +2.3% [0–3%]), with no evidence of edema, contrasting with deterioration in SCS controls. Venous lactate rose modestly but plateaued within physiologic range. Indocyanine green angiography confirmed uniform perfusion, and histology demonstrated preserved skin architecture without necrosis or significant apoptosis.

Conclusions: Normothermic EVP using HBOC-201 preserved porcine abdominal flaps for 24 h while maintaining physiologic stability, minimizing edema, and sustaining microvascular integrity. Compared to SCS, EVP significantly extends VCA preservation and may improve clinical feasibility in reconstructive transplantation.

INTERLEUKIN-6-DRIVEN PHENOTYPIC RESPONSES OF EPICARDIAL ADIPOSE TISSUE-DERIVED STEM CELLS IN CARDIAC ISCHEMIA

D.S. Vayser, S. Mukadam, F.G. Thankam.
Western University of Health Sciences College of Osteopathic Medicine of the Pacific, Pomona, California, UNITED STATES|

ABSTRACT BODY:

Purpose of Study: Interleukin-6 (IL6) is a pro-inflammatory cytokine implicated in myocardial ischemia (MI) and reperfusion injury. IL6 accumulation following MI stimulates the paracrine signaling in the adjacent epicardial adipose tissue (EAT), which in turn triggers EAT-derived stem cells (EATDS). Our previous research reported inflammatory phenotypes of EATDS. However, IL6+EATDS expression dynamics and associated sub-populations remain unexplored, especially under ischemia challenge. Our objective is to decipher the expression of IL6 in ischemic EATDS and to characterize the IL6+EATDS sub-types based on their signature genes.

Methods Used: EATDS isolated from swine heart were used for this study. The study consists of three groups: Control, Ischemia (ISC), or Ischemia/Reperfusion (ISC/R) based on the respective treatment groups. The level of IL6 was quantified in these EATDS by Western blotting, quantitative PCR, and immunofluorescence (IF). Single-cell transcriptomic profiling was performed to identify IL6+EATDS subpopulations. Differential gene expression and pathway enrichment analyses were utilized to assess the signature genes and associated biological pathways.

Summary of Results: Western blot and qPCR demonstrated increased IL6 expression in ISC and ISC/R groups relative to the control and in IF. Single-cell analysis of IL6+EATDS revealed decreased density of fibroblast phenotypes under ischemic conditions, with conserved transcriptional programs across the groups. The proliferating IL6+EATDS sub-population, represented by the ISC group, was characterized by the upregulation of mitotic regulators (ASPM, CENPF, TOP2A, CCNB1) and downregulation of the monocarboxylate transporter protein gene SLC16A3. The ISC/R group preserved this proliferative program; however, it shifted toward metabolic and nucleotide biosynthesis pathways. IL6+EATDS stromal cells subpopulation also peaked in ISC, with a significant upregulation of SELENBP1 (anti-oxidant responsive gene).

Conclusions: IL6 expression was elevated under ischemic stress in EATDS. IL6+EATDS fibroblasts remain the predominant sub-population, whereas proliferating and stromal cells subpopulations demonstrated divergent responses under ischemia and reperfusion. Our findings revealed that IL6 drives multiple sub-phenotypes of EATDS, suggesting their diverse role in cardiac ischemia. Further understanding with these sub-populations would unveil novel mechanistic insights into ischemic pathology.

CXCL10 MRNA UPREGULATION IN UV-EXPOSED RYR-R4456C MICE REVEALS CALCIUM-DEPENDENT MODULATION OF STING SIGNALING

M. Dulkanchainun[1], A. Shahid[2], Y. Huang[2].

[1]College of Osteopathic Medicine of the Pacific, Western University of Health Sciences, Pomona, California, UNITED STATES|

[2]Department of Biotechnology and Pharmaceutical Sciences, Western University of Health Sciences, Pomona, California, UNITED STATES|

ABSTRACT BODY:

Purpose of Study: The type 2 ryanodine receptor (RyR2) is a key calcium-release channel on the sarcoplasmic reticulum of cardiomyocytes; however, its functions in non-cardiac tissues are still not fully understood. The RyR2 R4497C mutation, one of the earliest variants found in patients with catecholaminergic polymorphic ventricular tachycardia (CPVT), increases the channel's open probability, leading to excessive calcium leak inside the cell. This disrupted calcium regulation makes cells more sensitive to stress and may influence downstream signaling pathways. Understanding how RyR2 mutations affect calcium dynamics outside the heart could offer new insights into stress responses and related diseases. Ultraviolet (UV) radiation damages DNA and activates innate immune responses via the stimulator of interferon genes (STING) pathway. STING detects cytosolic DNA and promotes type I interferon–stimulated genes, such as CXCL10, a pathway marker. While well-studied in DNA damage and immune signaling, the modulation of this pathway by abnormal calcium release is less understood. This study investigates whether UV exposure in RyR-R4456C mice increases STING activity, indicated by CXCL10 expression.

Methods Used: We used wild-type (WT) mice and mice with the RyR2 R4496C mutation (which corresponds to the human R4497C variant) as knock-in heterozygotes. We collected skin samples 48 hours after exposure to UV radiation, along with unexposed controls (n = 5 per group). We then extracted total RNA and analyzed transcriptomic profiles using RNA sequencing. We validated CXCL10 expression using quantitative reverse transcription PCR (RTqPCR).

Summary of Results: RNA sequencing revealed that UV exposure markedly upregulated multiple STING pathway genes, including CXCL10, Isg15, Mx1, Oas1a, Irf3, Cgas, Sting1, and Ifnar1, in RC mice compared with WT controls. Quantitative RT-PCR confirmed significantly elevated CXCL10 expression in UV-exposed RC skin relative to both UVexposed WT and unexposed controls (*p = 0.0205).

Conclusions: Our findings show that prolonged calcium release caused by the R4496C mutation increases innate immune activation under UV by enhancing the STING pathway. The notable increase in CXCL10 in UV-exposed RC mice suggests a mechanistic link between altered calcium dynamics and STING-driven immune signaling in response to genotoxic stress. In future studies, we will identify the specific immune cell populations responsible for CXCL10 production using immunofluorescence and flow cytometry.

RYR2 AND PHOSPHO-ERK EXPRESSION IN SKIN CANCERS

M. McKerahan[1], A. Shahid[2], C. Rathnayaka[2], Y. Huang[2].

[1]Western University of Health Sciences College of Osteopathic Medicine of the Pacific, Pomona, California, UNITED STATES|

[2]Western University of Health Sciences College of Pharmacy, Pomona, California, UNITED STATES|

ABSTRACT BODY:

Purpose of Study: There is a growing body of evidence that the antihypertensive drug carvedilol has many capabilities beyond the cardiovascular realm, i.e., preventing skin cancer. Activation of the MAPK pathway has been known as a central player in UV-induced skin cancer. Our preliminary studies suggest that carvedilol blocks MAPK mediated epidermal malignant transformation by antagonizing ryanodine receptor 2 (RyR2), which is a calcium (Ca2+) channel expressed on the endoplasmic/sarcoplasmic reticulum. In the heart, under the stress condition, RyR2 becomes a "leaky" Ca2+ channel, which is known as a mechanism for heart failure and cardiac arrhythmias. RyR2 is also expressed in the skin, where its function is more ambiguous. The normal RyR2 in skin cells is not a "leaky" receptor, however it appears that physical stressors such as UV can cause the channel to become leaky, leading to an increase in concentration of intracellular Ca2+. The goal of this project is to evaluate the correlation of expression of phospho-ERK (pERK), the active form of MAPK, and RyR2 in human skin tumors.

Methods Used: A tissue microarray containing 18 human squamous cell carcinomas (SCC) and 21 melanomas was purchased from TissueArray LLC and processed via immunohistochemistry (IHC) using antibodies for pERK and RyR2. Once stained, the samples were imaged under light microscopy for qualitative analysis using Fiji software. Expression scores were calculated to obtain the mean intensity of RyR2 and pERK staining in each tissue spot. Pearson's linear correlation coefficient r was calculated between RyR2 and pERK expression in SCC and melanoma samples using GraphPad Prism version 10.0.2.

Summary of Results: The IHC images demonstrate spatial co-localization of pERK and RyR2 in the same tumor areas in both SCC and melanoma. Scoring from the SCC spots identified a positive correlation between pERK and RyR2 (Pearson's r = 0.7171; 95% CI, 0.3761 to 0.8870). A positive correlation was also observed between pERK and RyR2 in melanoma (Pearson's r = 0.7412; 95% CI, 0.4552 to 0.8886).

Conclusions: These pilot human data, although with small sample sizes, support the hypothesis that MAPK/ERK activation may correlate with the RyR2 expression in human skin tumors.

CARDIAC FUNCTION IN ADOLESCENTS AND ADULTS BORN BEFORE NEWBORN SCREENING FOR CONGENITAL ADRENAL HYPERPLASIA

H. Selvakumar[1], J. Deterrich[2], B. Hoffman-Kipp[3], M.S. Kim[3], M. Geffner[4], S. Fuchs[5].

[1]Western University of Health Sciences, Pomona, California, UNITED STATES|

[2]Cardiology, Children's Hospital Los Angeles, Los Angeles, California, UNITED STATES|

[3]Center for Endocrinology, Diabetes and Metabolism, Children's Hospital Los Angeles, Los Angeles, California, UNITED STATES|

[4]Department of Pediatrics Center for Endocrinology, Diabetes and Metabolism, Children's Hospital Los Angeles, Los Angeles, California, UNITED STATES|

[5]Biomedical Sciences, Western University of Health Sciences, Pomona, California, UNITED STATES|

ABSTRACT BODY:

Purpose of Study: Congenital adrenal hyperplasia (CAH) is a potentially life-threatening condition caused by cortisol and aldosterone deficiencies, with excess androgen excess from impaired steroidogenesis. Newborn screening for CAH, introduced in California in 2005, enables early detection and treatment. However, those born before the implementation of screening, particularly males, were at increased risk of delayed diagnosis, potentially impacting cardiac function. CAH is a high-risk condition for cardiometabolic risk which emerges in childhood, including early onset obesity, hypertension, and dyslipidemia. Most cardiac function studies in CAH rely on echocardiography, which could miss early changes that predispose to cardiovascular disease. We evaluated cardiac function in adolescents and adults with CAH using cardiac MRI, and compared volumetric data with a normative population.

Methods Used: A cross-sectional study of cardiac function was performed in 16 adolescents and adults (15-30 yr; 5 females; 11 salt-wasting, 5 simple-virilizing form) with classical CAH due to 21-hydroxylase deficiency, who were born before newborn screening. Participants had an MRI (Phillips, 3T) at CHLA to evaluate cardiac parameters including: ventricular End-Diastolic Volume (EDV), End-Systolic Volume (ESV), Stroke Volume (SV), Ejection Fraction (EF), Left Atrial Volume (LAV), and Left Ventricular Mass (LVM). Data are presented as mean Z-scores calculated from normative population data (Rchsd.org/zscore). Z-tests were used to evaluate differences in cardiac function between patients with CAH (total, pediatric, and adult) and normative population means.

Summary of Results: Patients with CAH exhibited decreased Right SV (-0.76, $p = 0.02$) and increased LVM (0.99, $p < 0.01$), with preservation of systolic function, compared to the normative population mean; there were no significant differences in other cardiac measures. Adults (19-30 yr) with CAH exhibited decreased Right SV (-0.91, $p = 0.02$) and increased LVM (0.54, $p = 0.02$), while adolescents (15-18 yr) with CAH exhibited increased Right ESV (0.34, $p < 0.05$).

Conclusions: Patients with classical CAH born prior to newborn screening exhibit differences in Right SV and LVM compared to the normative population. This suggests that systolic function is preserved, but the myocardium may have structural changes that warrant further assessment for myocardial fibrosis or edema in CAH, especially as these changes can be seen with chronic hypertension and obesity.

HYPERGLYCEMIA REGULATES THE EXPRESSION OF MAPK13 AND THROMBOSPONDIN-1 REGULATING ANGIOGENESIS AND INFLAMMATION

T.B. Tran[1], J. Patel[2], V.N. Ho[2], V. Rai[1,2].

[1]Western University of Health Sciences College of Osteopathic Medicine of the Pacific, Pomona, California, UNITED STATES|

[2]Western University of Health Sciences, Pomona, California, UNITED STATES|

ABSTRACT BODY:

Purpose of Study: Diabetic foot ulcers (DFUs) are a major complication of diabetes, affecting 19-34% of diabetic patients in their lifetime. Despite the existing treatment, recurrence and amputation remain a major concern, highlighting the need for more effective therapies. Decreased angiogenesis, altered extracellular matrix (ECM) remodeling, and chronic inflammation underlie the pathophysiology of nonhealing DFU. Our previous RNA sequencing shows increased expression of MAPK13 in DFU tissue. Furthermore, previous network analysis revealed interactions between MAPK13, which regulates matrix remodeling and promotes inflammation, CXCR2, an IL-8 receptor that drives inflammation, and thrombospondin-1 (TSP-1), which inhibits angiogenesis. We hypothesized that hyperglycemia increases the expression of MAPK13, CXCR2, and TSP-1, together contributing to nonhealing DFUs.

Methods Used: Type 2 diabetes was induced in high fat fed Sprague Dawley rats using low dose streptozotocin. Cutaneous wounds were created on the dorsum of control and diabetic rats. Tissue samples were collected during and after wound healing (n = 7 per group; total = 28) and used in this study for investigating the gene and protein expression of MAPK13, CXCR2, and TSP-1 in normal and healed skin using RT-qPCR and immunostaining.

Summary of Results: H&E staining identified ulcerations in both control and diabetic tissue, as well as healed tissue in healed groups. RT-qPCR analysis showed increased expression of CXCR2 ($p=0.02$), MAPK13 ($p=0.005$), and TSP-1 ($p=0.0014$) in healed tissues compared to normal skin in control rats. In contrast, diabetic rats showed significantly increased TSP-1 expression ($p=0.009$), decreased MAPK13 ($p=0.005$), and comparable CXCR expressions in healed tissue compared to normal skin from diabetic rats. Comparison of healed tissues in control versus diabetic rats revealed increased CXCR2 and TSP-1 but lower MAPK13 expression. Immunostaining of tissue section for these proteins were analyzed using ImageJ and corroborated these findings.

Conclusions: Our results suggest that expression of CXCR2 and TSP-1 was increased and MAPK13 was decreased in healed tissues in the rat model of diabetes. Our results provide potential insight into impaired healing in diabetic wounds and highlight therapeutic targets for chronic DFUs by targeting angiogenesis, ECM remodeling, and chronic inflammation.

CONSIDERATION OF PULMONARY EMBOLISM IN WORSENING DYSPNEA AMONG PATIENTS WITH CONGESTIVE HEART FAILURE

P. Kasmai[1], J.M. Sugino[2].

[1]Western University of Health Sciences College of Osteopathic Medicine of the Pacific, Pomona, California, UNITED STATES|

[2]Providence Mission Hospital Mission Viejo, Mission Viejo, California, UNITED STATES|

ABSTRACT BODY:

Case Report: Dyspnea accounts for a considerable number of emergency room visits and subsequent hospital admissions. Congestive heart failure (CHF) and chronic obstructive pulmonary disease (COPD) are among the mostfrequent causes, accounting for 32% and 39% of cases, respectively.

An 86-year-old female presented to the hospital with progressive dyspnea for two days. She had a history of COPD, pulmonary fibrosis, combined systolic and diastolic heart failure with ejection fraction (EF) of 40%. Her medications included Aspirin, Carvedilol, Lasix, Spironolactone, Valsartan, a fluticasone-umeclidinium-vilanterol inhaler, and an albuterol nebulizer. Significant vital signs included a heart rate of 96 beats per minute, a respiratory rate of 22 breaths per minute and an oxygen saturation of 88% on room air. She had bibasilar crackles in her lungs and trace leg edema. BNP was 1700pg/ml. Chest radiograph revealed basilar atelectasis, right upper and left lower lung scar.

Electrocardiogram revealed sinus tachycardia without acute ischemic changes. Echocardiogram revealed EF of 41%, grade I diastolic dysfunction, moderate tricuspid valve regurgitation and right ventricular systolic pressure was 59 mmHg.

Given her history of CHF, presence of crackles and elevated BNP, she was initially treated with intravenous furosemide for suspected CHF exacerbation; however, her condition deteriorated. Her oxygen requirement increased from 3L/min to 30L/min via high-flow nasal canula by hospital day 4. Repeat BNP on day 4 rose to 4700 pg/ml. At this point, a CT pulmonary angiography was obtained that revealed bilateral lower lobe subsegmental pulmonary emboli, upper lobe emphysema, atelectasis and scarring in both lower lobes. A heparin infusion for treatment of PE started. By day 6, her dyspnea improved significantly, and her oxygen requirement decreased to 4L/min.

This clinical case emphasizes the importance of differential diagnosis in patients presenting with dyspnea. Although elevated BNP levels are commonly used to diagnose CHF exacerbation, they may also be seen in other conditions such as PE and right ventricular strain. In this patient, despite a history of CHF and elevated BNP, the absence of pulmonary congestion on CXR and significant fluid overload warranted further evaluation, ultimately resulting in the diagnosis of PE. Maintaining a broad differential is critical in patients presenting with dyspnea to prevent misdiagnosis and ensure timely recognition of pulmonary embolism.

EVALUATING AN AMPHIPATHIC CYCLIC PEPTIDE [W4R5] FOR ANTISCHISTOSOMAL ACTIVITY AGAINST SCHISTOSOMA MANSONI

E.G. Araujo, S. Natarajan, J. Spaan, M. Steinauer, R. Tiwari.
Western University of Health Sciences, Pomona, California, UNITED STATES|

ABSTRACT BODY:

Purpose of Study: Schistosomiasis infected over 260 million people in 2022 with over 10,000 succumbing to the illness annually. The most used anti-schistosome drug is Praziquantel (PZQ), however, there is growing evidence that Schistosoma mansoni might be developing a resistance to PZQ. PZQ also has limited efficacy on sexually immature worms, where for about 5 weeks post-exposure PZQ is ineffective. [W4R5] is a cyclic antimicrobial peptide with broad spectrum activity, membrane-disruptive properties. We hypothesized that [W4R5] exhibits antiparasitic activity against S. mansoni, potentially by disrupting parasite membranes, and therefore could complement or enhance current PZQbased therapy.

Methods Used: In vitro trials of [W4R5]'s efficacy was tested on schistosomes perfused from mice. Juvenile worms were collected at 26 days post-infection, and adult worms at 41 days post-infection. Schistosomes were divided into groups that received [W4R5] at concentrations of 0, 5, 10 and 15μM. To observe motility schistosomes were videotaped at multiple time intervals by a blinded observer. Death was confirmed via lack of motility and membrane disruption by presence of staining. Surivival and staining between concentration groups was compared using a logrank test and generalized linear regression model respectively.

Summary of Results: There was no significant difference in survival between the treatment groups for juveniles; however, adults receiving 15μM had a significantly lower survival probability than the controls and lower concentration groups. For juveniles, the predicted probability for the control group to stain was significantly lower than all other treatment groups. There were no differences in staining between the other three treatment groups for juveniles. For adults, the predicted probability for the 15μM group to stain was significantly higher than all other treatment groups. Across all concentrations, there was no difference in the predicted probability of staining between adults and juveniles.

Conclusions: In vitro, [W4R5] was effective at 15μM in killing adult S. mansoni, but not at the lower concentrations tested. [W4R5] did not kill juveniles at tested concentrations, but it increased membrane permeability, suggesting a membrane-disruptive mechanism. These findings support further evaluation of [W4R5] in dose–response and time-kill studies and as a potential adjuvant to PZQ –particularly to target juvenile stages–and in combination/synergy assays followed by in vivo validation.

IMMEDIATE RESPONSE OF TENOCYTES TO HYPOXIA DRIVES THE DOWNREGULATION OF MATRIX ASSOCIATED GENES

T. Eskandar[1], K. Vartanian[1], F.G. Thankam[2].

[1]Western University of Health Sciences College of Osteopathic Medicine of the Pacific, Pomona, California, UNITED STATES|

[2]Western University of Health Sciences, Pomona, California, UNITED STATES|

ABSTRACT BODY:

Purpose of Study: Hypoxia has been the initial pathological trigger associated with shoulder tendon injury (STI). Tenocytes are the major tendon cells involved in matrix homeostasis and the tolerance of tenocytes to hypoxic insults remains understudied. Logically, tenocytes elicit protective effects by altering expression of genes involved in tendon matrix homeostasis, especially by restoring the Collagen-I (COLI) to Collagen-III (COLIII) ratio. We hypothesize that hypoxic episodes alter the genes involved in tendon homeostasis. We aim to assess the status of COLI and COLIII along with key regenerative genes in swine tenocytes cultured under hypoxic conditions.

Methods Used: Swine shoulder tenocytes were cultured under 1% oxygen (hypoxia) for 24 hrs. Cell viability was assessed by MTT assay and microscopic morphometry. Tendon biomarkers included COLI, COLIII, and Scleraxis (SCX), while mesenchymal markers included Vimentin 1 (VIM1), fibroblast activation protein 1 (FAP1), and hypoxia-induced factor 1A (HIF1A). Expression level was determined at the transcript and protein level using qRT-PCR and immunostaining following standard protocols. Tenocytes cultured under normoxic conditions served as control.

Summary of Results: Tenocyte viability decreased considerably in the hypoxic treatment compared to control by 75.4±7.3%. The hypoxic tenocytes displayed significant alterations in morphology, displaying an oval-to-round appearance against the spindle and elongated morphology exhibited by control cells. The expression level of the mediators was altered at the transcript levels. SCX, COLI, and COLIII were downregulated in hypoxic conditions while HIF1A, VIM and FAP were upregulated in hypoxic conditions. Transcript analysis revealed a -4.65±0.543-fold decrease in SCX, -3.87±0.543-fold decrease in COLI, and -2.45±0.187-fold decrease in COLIII. HIF1A, VIM, and FAP displayed a similar increase. Immunostaining revealed a statistically significant decrease in HIF1A ($P<0.0005$) and an increase in VIM ($P<0.0005$) following hypoxia treatment. The COLI:COLIII ratio increased ~2-fold in hypoxia (1.025) compared to control (0.518).

Conclusions: Tenocytes respond to hypoxia by altering expression of ECM components and regenerative genes, such as restoring the COLI:COLIII ratio. Further understanding regarding the molecular signaling underlying the hypoxic response in tenocytes would open novel translational opportunities for early-stage management of tendon injury.

LIPOSOMAL GLUTATHIONE SUPPRESSES MYCOBACTERIUM AVIUM INFECTION IN A MICE MODEL OF MENINGITIS

I.H. Era, E. Sharma, K.C. Sasaninia, J. Melendez, N. Newman, W. Akif, K. Lutfy, V. Venketaraman.
Western University of Health Sciences, Pomona, California, UNITED STATES|

ABSTRACT BODY:

Purpose of Study: Tuberculous Meningitis (TBM) is the most severe form of extrapulmonary tuberculosis (TB) and is associated with immense morbidity and mortality worldwide. Individuals with TBM show a marked deficiency in glutathione (GSH) levels, the principal non-protein mechanism for maintaining the intracellular redox balance. Our lab has previously reported that GSH has direct antimycobacterial activity in vitro and in the lungs. Furthermore, we have shown that GSH deficiency in the lungs increased M. tb burden, while GSH replenishment improved the control of M. tb infection. Therefore, in vivo trials were conducted to determine what effect liposomal glutathione (LGSH) supplementation would have on the mycobacteria and the immune system of mice infected intraventricularly with M. avium. M. avium is a less virulent mycobacteria that is closely related to M. tb and contributes to significant morbidity in immunocompromised patients.

Methods Used: 15 C57BL/6 mice divided into three groups (6 infected mice, 6 infected+GSH mice, and 3 infected+diethyl maleate (DEM)) were infected intraventricularly with M. avium and sacrificed at 30 days. Mice organs were harvested, and brain lysates were plated on 7H11 agar plates. Tissue samples were also used for histological examination, ROS assays, and qPCR.

Summary of Results: 1. Bacterial counts showed that LGSH (40mM) treatment caused a significant reduction in the M. avium viability in the brain tissue when compared to the untreated control. In contrast, DEM-treatment (50mM) caused a significant increase in the M. avium burden.

2. qPCR showed that M. avium 16sRNA, NRF2, and IL6 were repressed in the LGSH group as compared to the infection control. However, these same bacterial markers and important markers of inflammation were increased in the DEM group.

Conclusions: This is the first study showing that LGSH supplementation significantly reduces infection and inflammatory burden in mice with intracerebral mycobacterium infection. Low bacterial counts from the brain tissue in the LGSH group show that LGSH may have direct bactericidal properties in vivo along with a role in replenishing stores of endogenous GSH depleted over chronic infection. This is further supported by the poor prognosis of DEM mice as DEM is a chemical depletor of GSH. LGSH mice had less 16sRNA and NRF2 expression showing a lack of pathogen and accompanying inflammatory process. Further studies with M. tb are warranted.

CASE REPORT: MANIA WITH PSYCHOTIC SYMPTOMS IN AN ADOLESCENT PATIENT ASSOCIATED WITH ASHWAGANDHA USE

J. Gonzalez[1], A. Ho[2], T. Liwag[2], D. Wong[2], E. Fu[2], A. Phan[3].

[1]Western University of Health Sciences College of Osteopathic Medicine of the Pacific, Pomona, California, UNITED STATES|

[2]Psychiatry, Kaiser Permanente Southern California, Fontana, California, UNITED STATES|

[3]California State University Long Beach, Long Beach, California, UNITED STATES|

ABSTRACT BODY:

Case Report: In recent years, Withania somnifera (WS), known as “ashwagandha” has gained popularity as a medicinal herb used to treat various conditions including depression, anxiety, and insomnia. Its therapeutic effects are attributed to a group of natural compounds known as withanolides.

We present a case of a 15-year-old female who had sudden onset of manic symptoms with psychotic features possibly precipitated by WS use. The patient took approximately 59 gummies of 200mg WS over 10 days (~12,000mg total dose) to help with mood and anxiety. She developed an acute onset of insomnia, social withdrawal, disorganized behavior, heightened anxiety, paranoia and racing thoughts.

Initially, the patient was diagnosed with depression with brief psychosis in the ED, and discharged home, but her symptoms worsened. She was later admitted to an inpatient psychiatric facility, treated for brief psychotic disorder and catatonia, and showed partial improvement. At outpatient follow-up, she continued to experience paranoia, thought blocking, and mood lability, which are symptoms of acute mania with psychotic features. A positive maternal history of bipolar I disorder suggests possible genetic predisposition, potentially unmasked or worsened by WS use.

This case report highlights the importance of screening for herbal supplement use in pediatric patients. Biochemical studies suggest that withanolides act on GABAA, GABAB and serotonin receptors, mimicking the effect of antidepressants. Antidepressant monotherapy is known to increase the risk of mania in bipolar patients. Despite only 1–3% of minors being formally diagnosed with mood disorders, more than 50% of parents provide supplements to their children, ~37% without medical guidance. Given there is limited evidence of WS safety/efficacy in mental health, it should be used with extreme caution, as high doses may exacerbate underlying psychiatric conditions.

THE PHARMACOLOGIC APPLICATION OF AMORPHOUS SOLID DISPERSIONS AND CIRCUMINOIDS.

M. Issar, A. Boyadzhyan, Y. Rabiei.
Western University of Health Sciences, Pomona, California, UNITED STATES|

ABSTRACT BODY:

Purpose of Study: The well known spice Turmeric (Curcuma longa) contains powerful polyphenols known as curcuminoids, which have become the subject of investigation in recent years. Namely, curcuminoids have been shown to play a role against a multitude of diseases likely due to their effects on numerous signaling molecules such as STAT3, cyclooxygenase-2, and C-reactive protein. With regards to Alzheimer's disease, Curcumin has served as a fluorescent probe for detecting β-amyloid plaques, but its application is constrained by low bioavailability. Despite their broad pharmacological activity, curcuminoids oral use is limited by very poor solubility, chemical instability, and rapid metabolism. Self-emulsifying drug delivery systems (SEDDS) are one approach to enhancing dispersion and solubilization in the gastrointestinal tract. The ability of SEDDS to retain the drug in solution depends on both the drug load and whether supersaturation can be maintained during digestion. The addition of amorphous solid dispersion (ASD) excipients is one strategy to reduce precipitation.

Methods Used: In this work, two curcuminoid-SEDDS were tested in an in-vitro lipolysis model: F15 (lower load) and F16 (higher load), each with or without ASD. Aqueous phase concentrations were measured after dispersion (T0) and during digestion (20–60 min). Data sets were analyzed as a percentage of the maximum theoretical solubilization (APMAX) and as integrated supersaturation ratios (SM = AUC{AP}/AUC{reference}).

Summary of Results: For the low-load system (F15), ASD conferred only a modest benefit: by 60 min, the solubilized fraction was ~31% compared to ~49% for F15ASD, with integrated SM{AUC} values of 0.64 and 0.60, respectively. For the higher-load system (F16), ASD gave a clear advantage: F16 maintained only ~25% solubilization at 60 min (SM{AUC} = 0.43), whereas F16ASD sustained ~56% solubilization with SM_{AUC} = 0.66.

Conclusions: This data emphasizes the dose-dependent relationship between ASD excipients and curcuminoid SEDDS as higher doses of ASDs enable supersaturation stability. This highlights the therapeutic and diagnostic potential of ASDs when used with curcumin, paving the way for future research into the broader medicinal benefits of curcuminoids.

THE β-BLOCKER CARVEDILOL INCREASES THE ANTITUMOR EFFICACY OF TAXANES IN DRUGRESISTANT CANCER CELLS

K. Lam[1], S. Yeung[2], Y. Huang[2].

[1]Western University of Health Sciences College of Osteopathic Medicine of the Pacific, Pomona, California, UNITED STATES|

[2]Western University of Health Sciences College of Pharmacy, Pomona, California, UNITED STATES|

ABSTRACT BODY:

Purpose of Study: Chemotherapy is the major treatment protocol utilized in treating and managing most forms of cancer. Despite its widespread use and efficacy, chemoresistance still poses a major obstacle in cancer treatment. Taxanes are one class of anticancer drugs that faces the issue of chemoresistance in various cancer types. The prostate cancer cell line, DU145-TxR, is resistant to taxanes including paclitaxel, docetaxel, and cabazitaxel. However, when combining the treatment of carvedilol with various taxanes, DU145-TxR cells have shown remarkably increased taxane sensitivity. Carvedilol is a β-AR receptor nonselective β-blocker and α1-AR blocker that is FDA approved for managing various cardiovascular conditions.

Methods Used: In this study, we verified the effects of carvedilol on taxane-resistance in different cancer cell lines. We utilized SRB assay, colony formation assay, apoptosis assay, and drug accumulation assay to analyze the effects of carvedilol and taxane in combination.

Summary of Results: In DU145-TxR cells, carvedilol increased paclitaxel-induced colony formation reduction and apoptosis, and intracellular accumulation of paclitaxel in a dose-dependent manner. Carvedilol also increased efficacy of paclitaxel and docetaxel in another docetaxel-resistant prostate cancer cell line PC3-TxR, and increased efficacy of paclitaxel in colon cancer cell lines CT26 (murine) and HT-15 (human). Carvedilol had no effect on paclitaxel cytotoxicity in human non-cancerous skin cell line HaCaT. As carvedilol is a racemic mixture consisting of 1:1 R- and S-carvedilol, the effects of R- and S-carvedilol enantiomers were tested separately on taxane-sensitivity in DU145-TxR cells. No differences were detected in the taxane sensitizing effects of R- and S-carvedilol compared to the racemic mixture of carvedilol. We also tested the effects of carvedilol combined with other chemotherapy drugs and found that carvedilol failed to sensitize cisplatin-resistant ovarian cancer cells to cisplatin. Carvedilol also failed to sensitize DU145-TxR to other chemotherapy drugs besides taxanes and doxorubicin. Other β-blockers were tested as well, demonstrating modest or no effects on taxane efficacy.

Conclusions: Based on our data, carvedilol increases the efficacy of taxanes and doxorubicin in taxane-resistant cancer cell lines independent of its β-AR and α1-AR blocking activity.

CCL5 KNOCKOUT INCREASES CFOS EXPRESSION AND MICROGLIA-NEURON INTERACTION

E. Chen[1], A. Leonor[1], I. Udoh[2], C. Shi[2], M. Zhou[2], Y. Shen[3].

[1]Western University of Health Sciences College of Osteopathic Medicine of the Pacific, Pomona, California, UNITED STATES|

[2]Western University of Health Sciences College of Dental Medicine, Pomona, California, UNITED STATES|

[3]University of California Los Angeles, Los Angeles, California, UNITED STATES|

ABSTRACT BODY:

Purpose of Study: The purpose of this project is to investigate whether neuronal CCL5 regulates memory allocation in the hippocampus and whether microglia are involved in this process. Memory allocation refers to how specific neurons are selected to encode a memory, a process influenced by neuronal excitability and cAMP response element-binding protein (CREB) activity. CCR5 (C-C chemokine receptor type 5), a receptor that inhibits CREB after activation, reduces the likelihood that a neuron will be recruited into a memory trace. One of its ligands, CCL5 (C-C motif chemokine ligand 5), is highly expressed in the hippocampus and may suppress memory allocation by activating CCR5. The precise role of CCL5 and its interactions with microglia in memory allocation remain unclear.

Methods Used: Combining the INTRSECT Cre-off/Flp-on system and Ccl5 conditional knockout (cKO) mice, hippocampal neurons were labeled with mCherry+ (Ccl5 cKO) and GFP+ (wild-type, or WT) in the same mouse. Then the mice were exposed in a novel context for 10 minutes, and 24h later were placed back in the same context for 5 min to recall the memory. 90 mins later, brains were collected and sliced at 50 μm using a vibratome. Immunostaining with c-Fos antibody was used to detect memory-allocated neurons. Confocal images were acquired from CA1 and dentate gyrus (DG) of the dorsal hippocampus (dHPC). c-Fos expression was quantified in GFP+ and mCherry+ neurons using Zen software. To assess microglia-neuron interaction, we stained slices with Iba1 and used Imaris software to quantify microglial volume overlap with GFP+ and mCherry+ neurons.

Summary of Results: There was a higher amount of mCherry+ than GFP+ neurons that co-expressed c-Fos in both the CA1 and DG regions of the dHPC. Quantification using Imaris also showed a significantly greater volume of intersection between microglia (Iba1+) and mCherry+ neurons compared to that between microglia and GFP+ neurons in both CA1 and DG.

Conclusions: Our results indicate that neurons with Ccl5 knockout were more likely to encode a memory than WT neurons. In addition, microglial-neuron interaction increased with Ccl5 knockout in neurons, which might be driven by heightened neuronal activity, as high c-Fos expression could signal microglia to engage in synaptic remodeling. Our results demonstrate that neuronal CCL5 regulates memory allocation and microglial-neuron interaction, which helps to elucidate the role of CCL5/CCR5 signaling in learning and memory.

CHARACTERIZATION OF COL6A1 KNOCKDOWN IN MOUSE HIPPOCAMPUS

L. Pillarisetti[1], W. Su[1], A. Saleh[1], M. Braga[2], M.B. Baudry[2], X. Bi[3].

[1]College of Osteopathic Medicine of the Pacific, Western University of Health Sciences, Pomona, California, UNITED STATES|

[2]Western University of Health Sciences, Pomona, California, UNITED STATES|

[3]Biomedical Sciences, Western University of Health Sciences, Pomona, California, UNITED STATES|

ABSTRACT BODY:

Purpose of Study: Evidence shows the extracellular matrix (ECM) plays critical roles in synaptic plasticity and memory function. We previously reported memory impairment in mouse models of Angelman syndrome (AS), a neurodevelopmental disorder, is associated with alterations in memory-related transcriptional regulation. In particular, memory recall-induced increase in expression of ECM genes, including collagen6α1 (COL6A1) observed in hippocampus from wildtype (WT) mice is absent in AS mice. To further determine the roles of COL6A1 in brain function, we used AAV shRNA-mediated knockdown (KD) of COL6A1 in hippocampus. This study focused on the characterization of COL6A1expression in hippocampus following COL6A1 KD.

Methods Used: Four weeks after AAV viral injection in ventral hippocampal CA1 region, brain tissues were collected. Cryosections (1 section/mouse, n=3 mice/group) were processed for immunofluorescence staining of COL6A1 and analyzed by confocal imaging across hippocampal subregions (CA1, CA3, DG); mCherry expression was used for assessment of viral infection. COL6A1 expression levels in shRNA KD mice were compared with scramble RNA (SC)-injected control mice. Additionally, six cells per section with different viral intensity were analyzed and level of viral infection was correlated with COL6A1 intensity at the cellular level. Statistical comparisons were made using unpaired t-tests and Pearson correlation.

Summary of Results: Clear expression of COL6A1 was observed in all hippocampal subregions, which agrees with the mRNA expression pattern published by the Allen Institute. Preliminary results showed that regional intensity of COL6A1 staining was not significantly different between SC and KD groups in CA1 ($p=0.527$), CA3 ($p=0.121$), or DG ($p=0.786$). However, there was a negative correlation between viral expression levels and COL6A1 levels in CA1 region in the KD group ($R2= 0.37$, $p=0.000347$), while a weak positive correlation was observed in the SC group ($R2 =0.12$, $p=0.000302$).

Conclusions: Results show significant COL6A1 expression in hippocampus, suggesting a potential role of COL6A1 in hippocampal function. For COL6A1 KD efficiency, COL6A1 levels did not significantly differ between the KD and SC groups at the regional level. COL6A1 intensity was negatively correlated with viral intensity in CA1 region in the KD group at the cellular level. Results imply that shRNA may have KD effects at the cellular level, but not at the regional level, indicating higher viral concentration and larger sample size are needed.

DOWNREGULATION OF FXR1 AND G3BP1 DISRUPTS STRESS GRANULE INTEGRITY AND ACTIVATES NLRP3 INFLAMMASOME UNDER METABOLIC STRESS

A. Pathak, H. Patel, R. Rajalekshmi, D.K. Agrawal
College of Osteopathic Medicine of the Pacific, Western University of Health Sciences, Pomona, California, UNITED STATES|

ABSTRACT BODY:

Purpose of Study: The stability of vascular immune homeostasis relies on stress granule (SG)-associated RNAbinding proteins such as FXR1 and G3BP1, which regulate inflammatory mediators post-transcriptionally. In metabolic disorders like hyperlipidemia (HL) and hyperglycemia (HG), disruption of this protective SG machinery may release the brake on NLRP3-caspase-1 (CASP1) inflammasome activity, accelerating carotid atherosclerosis.

Methods Used: Carotid artery tissues from Yucatan miniswine obtained via surgical procedure (control N=3, HL N=5 [hyperlipemia, 450-700 mg/dL cholesterol], HG N=5 [hyperglycemia, 100-250 mg/dL glucose]) were formalin-fixed, paraffin-embedded, and analyzed by hematoxylin-eosin and trichrome staining. The mRNA transcripts and protein expression of FXR1, G3BP1, NLRP3, and CASP1 were analyzed by RT-PCR and Western blotting. The cellular location of these proteins was defined by Immunohistochemistry.

Summary of Results: FXR1 transcripts were modestly increased in HL but decreased in HG; however, FXR1 protein expression was markedly reduced in both conditions, indicating translational repression or enhanced degradation. Similarly, G3BP1 mRNA was upregulated in HL (2.3-fold) and HG (8.5-fold), yet protein levels were consistently suppressed, confirming post-transcriptional dysregulation. This loss of SG regulators coincided with striking increases in the expression of NLRP3 inflammasome (421-fold in HL; 26-fold in HG) and CASP1 (21-fold in HL; 188-fold in HG). Western blotting demonstrated selective persistence of the 60 kDa NLRP3 isoform in HL/HG tissue, accompanied by cleaved CASP1 fragments (20/10 kDa), consistent with inflammasome activation. Immunohistochemistry localized NLRP3 and CASP1 to intimal macrophages within diseased arteries.

Conclusions: Downregulation of FXR1 and G3BP1 is a central molecular event in metabolic stress, leading to stress granule dysfunction and uncontrolled activation of the NLRP3-CASP1 inflammasome in the carotid artery. These findings identify the FXR1-G3BP1 axis as a potential therapeutic target to restore vascular immune homeostasis and prevent metabolic syndrome-associated atherosclerosis.

SEVERE SHORT STATURE IN AN ADOLESCENT MALE WITH LARON SYNDROME DUE TO A NOVEL GHR VARIANT: INITIAL RESPONSE TO RECOMBINANT IGF-1 AND AROMATASE-INHIBITOR TREATMENT

V.X. Yu[1,2], M. Geffner[2,3], A. Ryabets-Lienhard[2,3], L. Randolph[4], Z. Laron[5].

[1]Western University of Health Sciences, Pomona, California, UNITED STATES|

[2]Endocrinology, Diabetes, & Metabolism, Children's Hospital Los Angeles, Los Angeles, California, UNITED STATES|

[3]Keck Medicine of USC, Los Angeles, California, UNITED STATES|

[4]Medical Genetics, Children's Hospital Los Angeles, Los Angeles, California, UNITED STATES|

[5]Schneider Children's Medical Center of Israel, Petah Tikva, Center District, ISRAEL|

ABSTRACT BODY:

Case Report: Introduction: Laron syndrome (LS) is an ultra-rare autosomal-recessive disorder characterized by growth hormone (GH) resistance due to pathogenic variants in the gene encoding the GH receptor (GHR) typically involving its extracellular (EC) binding domain (exons 1-7), resulting in low GH-binding protein (GHBP) and IGF-1 levels. Patients exhibit severe short stature, distinctive facial features, obesity, and metabolic derangements. We present a unique case of an adolescent male with LS due to a novel homozygous variant in GHR exon 7 with normal GHBP levels and highlight his initial treatment course.

Case: An almost 16-yr-old male presented with severe, relatively proportional, short stature (height -7.06 SD, BMI 0.37 SD) (Fig. 1). He had an infantile face, depressed nasal bridge, high-pitched voice, blue sclerae, and delayed puberty [Tanner Stage (TS) 2, testosterone (T) 77 ng/dL (8-66), and bone age (BA) 12 yr]. Initial studies showed undetectable IGF-1 (<10 ng/mL, 201-609), low IGFBP-3 (0.8 mg/L, 3.5-10), normal peak stimulated GH (>10 ng/mL), and normal GHBP (1446 pmol/L, 290-3140) levels. IGF-1 generation test showed no response to GH (0.033 mg/kg/day x 7 days): mean IGF-1 11 ng/mL, 201-609; -5.5 SD, all clinically and biochemically consistent with LS. Genetic testing revealed a novel homozygous c.650T>G (p.Val217Gly) missense variant in exon 7 of the GHR that encodes the EC GH binding domain.

At 16.3 yr, puberty progressed to TS3. An aromatase-inhibitor was added (initially letrozole, then anastrozole due to high T) to delay epiphyseal fusion and augment growth potential. At 16.6 yr, rhIGF-1 (mecasermin) was started at 0.1 mg/kg daily and uptitrated to 0.12 mg/kg twice-daily. In the next 6 mo, his height improved from -7.1 to -6.82 SD with an annualized growth velocity of 15.6 cm/yr (Fig. 1). His BA progressed to 13 yr at actual age 16.9 yr. No hypoglycemia or other adverse effects were observed.

Conclusion: This unique case of severe LS involves a novel homozygous missense variant in the GHR affecting the EC GH binding domain and highlights the potential of meaningful linear growth in response to combined rhIGF-1 and aromatase-inhibitor treatment. Further follow-up is needed to evaluate the full effect of treatment on adult height. The presence of normal GHBP is unusual in LS but has rarely been seen in GHR variants involving EC binding domain. Functional studies are underway to further analyze this novel variant and implications on protein function.

MORPHOLOGICAL PREDICTORS OF OBSTRUCTIVE SLEEP APNEA SEVERITY ACROSS TREATMENT COHORTS

J. Garcia[1], A. Hardin[1], S. Ibrahim[2], A. Hardin[2].

[1]Western University of Health Sciences College of Osteopathic Medicine of the Pacific-Northwest, Lebanon, Oregon, UNITED STATES|

[2]Western University of Health Sciences College of Osteopathic Medicine of the Pacific, Pomona, California, UNITED STATES|

ABSTRACT BODY:

Purpose of Study: Obstructive sleep apnea (OSA) affects 5–10% globally and is characterized by recurrent airway collapse during sleep predicted by different etiologies including facial morphology and lifestyle. OSA contributes to cardiac, metabolic and inflammatory disease. This project examines OSA and identifies associations between severity measured by Apnea-Hypopnea index (AHI), type of treatment recommended, and variations in craniofacial structures.

Methods Used: Cone beam computed tomography (CBCT) scans were analyzed from two sets of individuals diagnosed with OSA: those undergoing maxillomandibular advancement (MMA) and distraction osteogenesis maxillary expansion (DOME). Three-dimensional landmarks capturing the shape of the mandible, maxilla, and airway were collected from CBCT scans (N = 14 MMA, 10 DOME). Parallel testing was used to ensure landmarking reliability between researchers. Principal Component Analysis (PCA) was used to identify axes of greatest variation in the samples. Relationships of principal components, centroid size, and linear dimensions with AHI, accounting for sex, were analyzed using generalized linear mixed modeling.

Summary of Results: There was substantial overlap in craniofacial morphology between individuals undergoing MMA and DOME. In the shape-based model, treatment type (MMA vs. DOME) and PC2 were significant predictors of AHI, while age was independently associated with severity ($p = 0.034$, $p = 0.046$, and $p = 0.002$, respectively). In contrast, traditional linear dimensions (posterior nasal spine to pharyngeal wall distance, palatal depth, mandibular height) did not demonstrate statistical significance. Sex was not associated with AHI in either model.

Conclusions: This study investigates craniofacial morphology in patients undergoing MMA versus DOME for treatment of OSA. Morphology related to airway dimensions were associated with OSA severity. However, we did not detect a clear distinction in craniofacial shape between patients selected for MMA and DOME. There is a critical gap in how obstructive sleep apnea treatment pathways are determined. Choices between MMA and DOME often rely on subjective or experience-based impressions rather than quantifiable craniofacial criteria. By linking craniofacial morphology to OSA severity, we aim to establish objective markers that guide treatment, enable earlier intervention, while reducing the cardiovascular, neurological, and quality-of-life burdens of the disease.

GROWING PAINS: A REDDIT-BASED THEMATIC ANALYSIS OF BODY IMAGE DURING PREGNANCY

S. Molla, L. Chheng, A.L. Nelson.
Western University of Health Sciences, Pomona, California, UNITED STATES|

ABSTRACT BODY:

Purpose of Study: Pregnancy is a period of significant physical and psychological change, and body image is a critical component of maternal health. Traditional methods such as surveys and interviews may be influenced by participants' awareness of being studied, potentially limiting the authenticity of responses. Reddit, as an anonymous social platform, provides access to unfiltered discussions. This study examines narratives on Reddit to gain deeper insight into body image experiences during pregnancy and to inform prenatal care.

Methods Used: We performed a thematic analysis of posts from 2020-2025 using the search words "bodily changes + pregnancy" and "body image + pregnancy", which led us to 10 pregnancy-related subreddits discussing body image changes in pregnancy. Posts and comments were included based on relevance, engagement (≥10 comments or ≥5 upvotes/replies), and English language. We extracted physical symptoms and associated attitudes, which were organized into broader themes (e.g., negative/positive esteem and body image, generalized surprise, humorous/sarcastic coping, loneliness, expected). The WesternU IRB determined this study does not constitute human subjects research.

Summary of Results: We analyzed 75 posts and 375 comments, yielding 548 symptom references. The most frequently discussed symptoms were weight gain (30.7%), general body changes (20.3%), and the baby bump (16.2%). Weight gain (64.9%) and general body changes (63.1%) were predominantly associated with negative esteem and body image, whereas the baby bump was more commonly associated with positive esteem and body image (56.2%). Overall, negative esteem/body image emerged as the most prevalent thematic category (55.1%), followed by positive esteem/body image (23.3%) and perceptions of expected changes (11.0%).

Conclusions: Our findings demonstrate that weight gain and generalized body changes were most frequently associated with negative esteem, whereas the baby bump was more often linked with positive esteem. Overall, negative body image attitudes predominated, suggesting that adverse perceptions of physical changes remain a salient concern during pregnancy. These results highlight the importance of prenatal education that proactively addresses expected bodily changes, enabling women to form realistic expectations and healthier attitudes.

HEALTH EQUITY AND REPRESENTATION IN ONLINE LONG COVID SUPPORT COMMUNITIES: A COMPARISON TO U.S CENSUS DATA

I. Bauman, C. Tong, A. Wong, M. Othman.
Western University of Health Sciences College of Osteopathic Medicine of the Pacific, Pomona, California, UNITED STATES|

ABSTRACT BODY:

Purpose of Study: In 2022, the CDC estimated that nearly one in five Americans who contracted COVID-19 developed Long COVID, a condition with no definitive cure. Social determinants of health may influence susceptibility to Long COVID. A 2022 U.S. Census survey found that women, Hispanic individuals, transgender participants, bisexual participants, and economically disadvantaged populations are disproportionately affected. To assess whether marginalized groups are adequately represented in online communities, we administered a questionnaire to members of a Reddit support forum.

Methods Used: An anonymous multiple-choice survey was created using Qualtrics, mirroring items from the 2022 U.S. Census Household Pulse Survey. Our inclusion criteria required participants to have had a positive COVID test and subsequently experienced long COVID symptoms for at least 3 months. Additionally, participants had to be at least 18 years old and live in the U.S. The questionnaire was active from December 20th, 2024, to September 12th, 2025. We chose to post this survey to r/CovidLonghaulers, a subreddit with over 67,000 members, due to the subreddits popularity and accessible interface. 46 Preliminary responses were analyzed and compared to national survey data.

Summary of Results: Among respondents who met inclusion criteria, 89% identified as white (vs. 29.9% Census), 72% did not have a pre-existing disability (vs. 16.7%), 96% were cisgender (vs. 51.5%), and 72% were heterosexual (vs. 30.0%). Furthermore, 72% had a bachelor's degree or higher (vs. 23.6%), ~ 50% reported household income ≥$100,000 (vs. 56.3%), and 63% were ≤39 years old (vs. 60.3%).

Conclusions: Marginalized groups disproportionately affected by Long COVID are potentially underrepresented in online support forums. These spaces are crucial to provide patient-to-patient support given the absence of effective treatment.

Cultural attitudes towards seeking help and disclosing personal information may contribute to a selection bias, thereby influencing who has a presence on these platforms and who may respond to demographic surveys. Due to the limited number of responses we received, we hope that future research will better reflect the utilization of online resources among minority populations and identify strategies to reduce barriers. Expanding inclusivity in digital communities may strengthen support and resilience for those living with chronic conditions.

INVESTIGATING OMIPALISIB AS A DUAL TOR COMPLEX 1/ TOR COMPLEX 2 INHIBITOR TO EXTEND YEAST LONGEVITY

K. Mittl, B. Wasko.
Western University of Health Sciences College of Osteopathic Medicine of the Pacific-Northwest, Lebanon, Oregon, UNITED STATES|

ABSTRACT BODY:

Purpose of Study: Rapamycin extends longevity of diverse species, from yeast to non-human primate models through selective inhibition of the TOR complex 1 (TORC1). However, it can also have off-target effects on TORC2, and the role of TORC2 in aging remains poorly defined. Omipalisib (GSK2126458) is a potent ATP-competitive inhibitor of TOR Complex 1 (TORC1), TORC2, and phosphoinositide 3-kinases (PI3Ks). This study aims to determine whether omipalisib extends yeast lifespan and seeks to investigate its molecular targets.

Methods Used: Saccharomyces cerevisiae (yeast) growth assays were conducted in 96-well plates containing standard YPD medium, incubated with shaking at 30 °C. The experiments utilized wild-type haploid yeast and a drug sensitive 12Δ strain lacking twelve genes associated with drug efflux. Chronological lifespan (CLS) assays in wildtype and drug-sensitive yeast strains treated with omipalisib (at sub-growth inhibitory concentrations), rapamycin, or control are in progress. In parallel, growth suppression screens are performed using inhibitory omipalisib concentrations. Drug resistant strains will undergo whole-genome sequencing to identify suppressor mutations and candidate molecular targets.

Summary of Results: At a concentration of 100 μM, omipalisib had minimal effect on the growth rate of a wild-type yeast strain. In contrast, the drug-sensitive 12Δ strain, exhibited complete growth inhibition at the same concentration, with significant impairment observed at concentrations as low as 1.25 μM. We hypothesize that omipalisib will extend chronological lifespan (CLS) and aim to investigate whether this effect is dependent on TORC1 signaling. Wholegenome sequencing of resistant mutants is expected to reveal mutations within the ATP-binding domains of TOR1, TOR2, and/or VPS34 (PI3K). However, the emergence of novel loci may provide broader insights into omipalisib's mechanism of action.

Conclusions: This work will provide the first evaluation of the effect of omipalisib on yeast aging. By integrating lifespan assays and genetic suppression analyses, the study will explore the contributions of TORC1 and TORC2 on longevity. The findings may guide the development of new therapeutic strategies for promoting longevity pathways in higher eukaryotes.

YOUTUBE AS A TOOL FOR DEMENTIA EDUCATION: A 7-YEAR ANALYSIS OF ENGAGEMENT AMONG OLDER CHINESE AMERICANS

C.Q. Yang[1], B.K. Woo[2,3].

[1]Western University of Health Sciences, Pomona, California, UNITED STATES|

[2]Chinese American Health Promotion Laboratory, University of California Los Angeles, Los Angeles, California, UNITED STATES|

[3]Department of Psychiatry and Biobehavioral Science, Olive View UCLA Medical Center, Sylmar, California, UNITED STATES|

ABSTRACT BODY:

Purpose of Study: In underserved populations, cultural and linguistic barriers to psychoeducation can perpetuate stigma, delay help-seeking, and worsen health disparities. This study examined how older Chinese Americans engaged with dementia education on YouTube, analyzing longitudinal viewing patterns and the platform's role in providing culturally adapted health information, with the aim of identifying strategies to improve outreach.

Methods Used: Two dementia psychoeducation videos recorded by a psychiatrist in Cantonese were uploaded to YouTube. Analytics from January 1, 2014 - December 31, 2020 were reviewed and divided into two 42-month intervals: "Period 1" (January 1, 2014 – June 30, 2017) and "Period 2" (July 1, 2017 – December 31, 2020). Analyses were limited to U.S.-based viewers aged ≥ 65 years old and included descriptive statistics, Poisson rate ratio, and chisquare tests.

Summary of Results: Across 7 years, the videos generated 41,310 views, 4,928.7 hours of watch time, and an average view duration of 7:09 minutes. 55% of views originated from suggested videos. Content was shared 1,238 times, with WhatsApp accounting for 60.5% of shares. Viewership more than doubled in Period 2 compared with Period 1 (27,933 vs. 13,377 views) with a significantly higher monthly viewing rate (665.1 vs. 318.5; $z = 70.02$, $p < .001$, RR = 2.09). Period 2 also had higher watch time compared with Period 1 (3,506.5 vs. 1,422.2 hours). Operating system usage shifted, $\chi2(2, N = 37,986) = 696.68$, $p < .001$, with increased Android and Windows use. Device usage patterns changed, $\chi2(3, N = 42,091) = 7176.48$, $p < .001$, with mobile phones and smart televisions (TVs) gaining traction while computer viewing declined. Suggested videos and browse features were traffic sources that became more influential drivers of engagement, $\chi2(4, N = 39,626) = 1118.59$, $p < .001$.

Conclusions: From 2014 to 2020, YouTube emerged as a useful tool for delivering culturally specific dementia education to older Chinese Americans, with viewership more than doubling alongside substantial changes in how content was accessed and engaged with. Results point to the increasing role of mobile devices, smart TVs, and algorithm-driven suggestions, as well as WhatsApp's prominence in sharing. Future outreach efforts should focus on optimizing videos for mobile and TV viewing, harnessing recommendation algorithms, and integrating culturally relevant sharing practices to broaden impact.

THE IMMUNOMODULATORY EFFECTS OF HYPERGLYCEMIA ON PRO-INFLAMMATORY CYTOKINES AND SURFACE RECEPTORS USING RAT MODELS OF DIABETES

V.N. Ho, T.B. Tran, J. Patel, V. Rai.
Western University of Health Sciences College of Osteopathic Medicine of the Pacific, Pomona, California, UNITED STATES|

ABSTRACT BODY:

Purpose of Study: Diabetic foot ulcers (DFUs) are a major cause of morbidity worldwide, along with the risk of other chronic health issues. Hyperglycemia disrupts immune regulation at the wound site and may contribute to non-healing DFUs. This study investigates the expression of CD36 (inflammation/angiogenesis), TLR7 and CD69 (immune regulation/inflammation), and PD-L1/CD274 (inflammation/tissue repair) in response to hyperglycemia using rat models of diabetes with cutaneous wounds. We hypothesized that the expression of CD36 and TLR-7, along with their target molecules CD274 and CD69, is upregulated in DFUs, leading to a local dysregulation that impairs wound healing. Understanding the molecular pathway of these surface receptors may provide essential insights into diabetic foot ulcer pathogenesis and identify potential therapeutic targets to enhance wound healing in diabetic patients.

Methods Used: Diabetes in Sprague Dawley rats was induced using low-dose streptozotocin injected intraperitoneally in rats on a high-fat diet. Rats were divided into four groups: not-healed control, healed control, not-healed diabetic, and healed diabetic. Skin samples from all groups were analyzed using Hematoxylin and Eosin (H&E), trichrome, and immunohistochemistry stains to evaluate histopathological changes. RT-qPCR was performed to assess mRNA expression. Student's t-test was used for statistical significance.

Summary of Results: H&E staining of healed diabetic wounds showed scar formation without sebaceous glands, sweat glands, and hair follicles. Trichrome stain showed decreased collagen content in the not-healed controls and diabetic wounds compared to the healed wounds, as evident by decreased blue color. The PCR results showed that CD36 was most significantly upregulated ($p < 0.0001$) in the healed diabetic group compared to other groups. When comparing to the control group, CD69 ($p < 0.001$) and CD274 ($p < 0.0001$) were both significantly upregulated in the healed control group. Lastly, TLR7 appears to be upregulated in all groups, with a significant increase ($p < 0.01$) in the diabetic healed group.

Conclusions: These findings suggest that CD36 and TLR7 may contribute to the wound healing response under hyperglycemia, while CD69 and CD274 were more associated with wound healing in normoglycemia. These findings highlight new insights into wound healing pathways under hyperglycemia and suggest that targeting these receptors may provide new therapeutic strategies for improving DFU outcomes.

DISRUPTION OF NERVE REGENERATION AND WOUND HEALING IN DIABETIC FOOT ULCERS

J. Patel, V.N. Ho, T.B. Tran, V. Rai.
Western University of Health Sciences College of Osteopathic Medicine of the Pacific, Pomona, California, UNITED STATES|

ABSTRACT BODY:

Purpose of Study: Diabetic foot ulcers (DFUs) are debilitating complications of diabetes, driven by impaired nerve regeneration and dysregulated inflammation. While nerve regeneration is crucial for wound healing and recurrence prevention, it is impaired by hyperglycemia. The mechanisms underlying this impairment remain unclear, making it important to investigate changes in key mediators of the healing process. Activin A supports neuronal repair by regulating inflammation and promoting progenitor differentiation, Synaptophysin marks synaptic remodeling during regeneration, and TNFRSF10B contributes to apoptosis and inflammatory signaling. This study aims to examine the effects of hyperglycemia on the expression of these markers using a rat model.

Methods Used: Type 2 diabetes was induced in Sprague Dawley rats through streptozotocin administration in a previous study. Animals were considered diabetic if tail vein blood glucose levels exceeded 250 mg/dL for at least 14 consecutive days. Cutaneous wounds were then created on the dorsal surface of both diabetic and control rats. Skin tissues were collected from control and diabetic rats in ulcerated skin and after healing (n=7 per group, total 28). These tissues were used to measure gene and protein expression of Activin A, Synaptophysin, and TNFRSF10B using RT-qPCR and immunohistochemistry. Hematoxylin and Eosin and Trichrome staining were used to illustrate the ulcers in the ulcerated skin and tissue repair in the healed skin.

Summary of Results: PCR analysis revealed that healing in control rats was associated with increased expression of Activin A, synaptophysin, and TNFRSF10B, whereas diabetic tissues failed to demonstrate similar induction. In diabetic-healed skin, regenerative and inflammatory markers were markedly reduced compared to controls. The protein expression measured from IHC analysis corroborated the gene expression findings, showing increased protein expression of all three mediators in control tissues compared to diabetic tissues. Histological staining portrayed ulceration in tissues and restored morphology in healed groups.

Conclusions: Hyperglycemia reduced the expression of key mediators involved in axonal regeneration, apoptosis, and inflammation. These findings connect the disruption of neuronal repair and inflammatory regulation under hyperglycemia to the pathogenesis of poor healing in DFUs. These molecular mediators may serve as potential targets for therapeutic interventions to promote nerve regeneration, angiogenesis, and regulate inflammation.

DEVELOPMENT OF A QUANTITATIVE ASSAY TO ASSESS THE REDOX ACTIVITY OF LIPASE MATURATION FACTOR -1

S. Rejali, M. Peterfy.
Western University of Health Sciences, Pomona, California, UNITED STATES|

ABSTRACT BODY:

Purpose of Study: Hypertriglyceridemia is a risk factor for cardiovascular disease, most often caused by impaired clearance of triglyceride-rich lipoproteins. Central to this pathway is lipoprotein lipase (LPL), which requires proper folding and activation in the endoplasmic reticulum (ER). Lipase Maturation Factor 1 (LMF1), an ER membrane protein, is essential for the post-translational maturation of LPL, yet the molecular mechanism by which LMF1 promotes LPL folding remains unclear. Emerging evidence suggests that LMF1 may affect ER redox homeostasis and facilitate the rearrangement of disulfide bonds during LPL biogenesis. The objectives of this study were to (1) develop a quantitative assay to assess LMF1 redox activity and (2) identify the structural determinants of LMF1 redox function.

Methods Used: We developed a dual luciferase assay using transfected LMF1-deficient HEK293 cells to monitor the impact of LMF1 on ER redox status. An engineered firefly luciferase containing multiple non-native cysteine residues was targeted to the ER as a redox-sensitive reporter, while Renilla luciferase served as a normalization control. The assay was optimized for transfected DNA amount, LMF1: reporter ratio and linearity. A panel of LMF1 deletion mutations were then analyzed to map the structural domains involved in LMF1 redox function.

Summary of Results: LMF1 expression increased firefly reporter activity in a dose-dependent manner, consistent with increased flux of electrons into the ER and a more reducing ER environment. The optimized assay involved the transfection of 500 ng DNA per 24-well at a 4:1 reporter-to-LMF1 plasmid ratio and resulted in a ~10-fold dynamic range with respect to LMF1. The analysis of deletion mutants revealed that several ER-luminal domains incrementally contributed to the redox activity of LMF1, but no single domain was required for its function.

Conclusions: We developed and validated a novel assay to measure the redox activity of LMF1 in the ER. Our results indicate that LMF1 possesses functionally redundant domains involved in redox activity and provide initial mechanistic insights into how LMF1 facilitates disulfide bond reduction during LPL folding. Furthermore, the assay developed in this work will allow the functional analysis of LMF1 mutations associated with hypertriglyceridemia in future studies. This work was supported by NIH grant HL154071.

INTEGRATION OF MANUAL AND LARGE LANGUAGE MODEL-BASED CURATION OF KINASE SUBSTRATE INTERACTION FUNCTIONALITY

Y. Hwang[1], G. Dela Cruz[1], [2]L. Amare[2], H. Lin[2], J. Coppé[2], K. Rivera Velez[3].

[1]Western University of Health Sciences College of Osteopathic Medicine of the Pacific-Northwest, Lebanon, Oregon, UNITED STATES|

[2]University of California San Francisco, San Francisco, California, UNITED STATES|

[3]Georgetown University, Washington, District of Columbia, UNITED STATES|

ABSTRACT BODY:

Purpose of Study: Aberrant kinase signaling is at the core of many diseases, such as cancers, and is therapeutically targetable. The PhosphoAtlas database is a kinase network resource that encompasses >15,700 phospho-catalytic protein-protein interactions. While PhosphoAtlas provides directional information on kinase-substrate circuits, it lacks critical information on the biological effects of individual interactions–i.e. activation/inhibition. As high throughput analyses are becoming increasingly crucial to understand complex mechanisms that involve cascades of inhibitory and activating events, we employed manual curation and a large language model (LLM) to extract the biological functions of kinase-substrate interactions from published literature. The purpose of this study is to integrate the outputs of these two methods, serving as a major update to PhosphoAtlas that will enable a deeper understanding of disease and more precise therapeutic target identification.

Methods Used: Biological functions for various kinase-substrate interactions were assessed using manual curation and the OpenAI GPT4 Turbo LLM. One hundred substrates were selected from UniProtKB, a curated protein database, and queried on UniProtKB using the LLM to summarize the biological effect of phosphorylation events involving the input substrates. For manual curation, the biological effects of the same events were manually curated from UniProtKB. Parameters, such as length of time to curate and final curated effect of the interaction, were compared between the two methods.

Summary of Results: From the LLM, five kinase-substrate interactions were found to have published evidence on UniProtKB. Time spent curating by the LLM averaged 24 seconds to query 100 entries (i.e. substrates), while that for the manual method ranged from 2-30 minutes depending on the number of publications for each interaction. After curating the biological effect using the two methods, four of the five interactions were found to be activating via both methods, while the BTLA-TNFRS14 Y61 interaction differed between the methods; while the LLM found it to be activating, manual curation found it to be inhibitory.

Conclusions: The use of an LLM significantly decreased the amount of time spent curating the biological effects of kinase-substrate interactions of interest. The manual and LLM methods yielded matching effects for a majority of interactions, but differed in one, highlighting the need to leverage the strengths of both methods while taking precaution of discrepancies.

PROTEIN ANALYSIS OF HEAD AND NECK SQUAMOUS CELL CARCINOMA XENOGRAFT TUMORS FOLLOWING BLUE LIGHT TREATMENT

S. Momi, A. Alam, P. Kaur, J. Lewis.
Western University of Health Sciences, Pomona, California, UNITED STATES|

ABSTRACT BODY:

Purpose of Study: Head and neck squamous cell carcinoma (HNSCC) represents ~90% of oropharyngeal cancers and remains associated with high morbidity and mortality despite advances in surgery, chemotherapy, and radiation. Few novel therapies have emerged in the past three decades. Previous in vitro work showed that exposing HNSCC cells to 400–500 nm blue light (BL) reduces viability, while normal oral keratinocytes (HOK) and gingival fibroblasts were unaffected. This study investigated whether these effects occur in an in vivo xenograft model and sought to identify BL-induced protein changes relevant to tumor growth.

Methods Used: UM-SCC-17B xenografts were established in nude (nu/nu) mice. Tumors were untreated (N=5) or treated daily with 90-second BL exposures (45 J/cm2; Bisco VIP curing unit; N=5). Tumors were measured daily in vivo with digital calipers. After 14 days, tumors were harvested, fixed for immunohistochemistry, or flash-frozen for protein analysis. Proteins (25 µg) were separated by SDS-PAGE, transferred to PVDF membranes, and probed for Ecadherin, IkappaB, and β-actin as a loading dose.

Summary of Results: UM-SCC-17B xenografts were established in nude (nu/nu) mice. Tumors were untreated (N=5) or treated daily with 90-second BL exposures (45 J/cm2; Bisco VIP curing unit; N=5). Tumors were measured daily in vivo with digital calipers. After 14 days, tumors were harvested, fixed for immunohistochemistry, or flash-frozen for protein analysis. Proteins (25 µg) were separated by SDS-PAGE, transferred to PVDF membranes, and probed for Ecadherin, IkappaB, and β-actin as a loading dose.

Conclusions: BL treatment significantly reduced xenograft growth and was associated with increased E-cadherin and IkappaB expression. These changes may reflect reduced proliferation, enhanced adhesion, and decreased invasiveness. Normal HOK and fibroblasts were unaffected, supporting safety in non-tumor tissue. Further studies are needed to define the molecular pathways underlying BL-mediated inhibition of HNSCC progression.

LATENT TUBERCULOSIS REACTIVATION FOLLOWING TREATMENT FOR PREOPERATIVE HEPARININDUCED THROMBOCYTOPENIA AND MECHANICAL MITRAL VALVE REPLACEMENT

D. Damron[1], N.E. Salm[1], J. Holland[2], A. Sahu[2], A. Doyle[3].

[1]Western University of Health Sciences, Pomona, California, UNITED STATES|

[2]University of Missouri-Kansas City, Kansas City, Missouri, UNITED STATES|

[3]Anesthesiology, Saint Luke's Health System Inc, Kansas City, Missouri, UNITED STATES|

ABSTRACT BODY:

Case Report: Tuberculosis (TB) remains the leading infectious cause of death worldwide, despite international efforts. Approximately 25% of the world population has a latent tuberculosis infection (LTBI), and 80% of new TB diagnoses in the US are due to reactivation. While the tuberculin skin test (TST) has high sensitivity for LTBI screening, newer screening methods are limited by modest sensitivity despite a higher level of specificity. Therefore, LTBI reactivation accounts for a significant number of active TB cases, highlighting the importance of screening, diagnosis, and treatment in high-risk patients/populations.

We present a case of a 50-year-old Asian female from Micronesia, who had a prolonged hospitalization for severe mitral regurgitation with WHO group 2 pulmonary hypertension and right ventricular failure, secondary to rheumatic heart disease, requiring mechanical mitral valve replacement. Her preoperative course was complicated by Serotonin release assay (SRA) negative heparin-induced thrombocytopenia (HIT), which was treated with plasmapheresis (PLEX) and perioperative intravenous immunoglobulin (IVIg). Post-operatively, the patient experienced recurrent fevers and acute hypoxic respiratory failure requiring reintubation and tracheostomy. Despite empiric treatment for suspected ventilator-associated pneumonia (VAP) and confirmed Mycoplasma pneumonia with doxycycline, her recurrent fevers persisted. One week after discharge, she was readmitted for tracheostomy site bleeding. A chest computed tomography (CT) scan for persistent fevers not responding to antibiotics revealed findings consistent with miliary TB. Subsequent sputum and CSF cultures/polymerase chain reaction confirmed diagnoses of pulmonary TB and TB meningitis. Abdominal imaging and colonoscopy demonstrated a psoas abscess and possible ileocecal TB. Anti-tubercular and steroid therapy initially provided positive outcomes. However, appropriate anticoagulation was hindered by recurring arterial GI bleeds in the setting of suspected ileocecal TB.

This case illustrates the importance and potential benefit of infectious disease screening in high-risk LTBI patients from TB endemic areas before undergoing immunosuppressive therapies or cardiopulmonary bypass. Early consideration, identification, and intervention of LTBI may help prevent devastating outcomes secondary to TB reactivation.

EXPLORING THE RELATIONSHIP BETWEEN ALCOHOL USE AND TRAUMA OUTCOMES IN PEDIATRIC TRAUMA PATIENTS POST-COVID-19 PANDEMIC

A.M. Zayed[1], A. Henken-Siefken[2], A. McCague[3].

[1]College of Osteopathic Medicine of the Pacific, Western University of Health Sciences, Pomona, California, UNITED STATES|

[2]Desert Regional Medical Center, Palm Springs, California, UNITED STATES|

[3]Surgery, Desert Regional Medical Center, Palm Springs, California, UNITED STATES|

ABSTRACT BODY:

Purpose of Study: This retrospective study explores the association between alcohol use, demographics, and trauma outcomes in pediatric patients between 2022-2023. Outcomes included ICU length of stay (LOS), mortality rate, ventilator days, Glasgow Coma Score (GCS), assisted respiration, and injury severity score (ISS). Given that alcohol use among youth patients has increased since the COVID-19 pandemic, the primary objective of this study is to investigate alcohol use and its relationship to trauma outcomes in pediatric patients in the U.S. post-pandemic.

Methods Used: The study used pediatric patient records from the National Trauma Data Standard. Patients were included in analysis if they were 15 years old or younger, and if they were given an alcohol screening. Patients were divided into Blood Alcohol Content (BAC)<0.08 g/dL and BAC≥0.08 g/dL groups. Mean LOS, GCS, ISS, ventilator days, mortality rate, and assisted respiration were compared, and odds ratios were calculated for mortality and suffering major trauma events. An ISS>15 denoted “major trauma” and a GCS≤0.08 indicated high probability of coma. Data analysis was done in Microsoft Excel 2025, with a significance threshold of $p<0.001$. Chi-Square tests were performed for categorical variables. Two-tailed t-tests were performed for continuous variables.

Summary of Results: 183,943 pediatric patients were admitted to a trauma center between 2022-2023. Of these, 44269 patients were screened for alcohol use, with 36985 patients with BAC<0.08 g/dL and 7284 patients with BAC≥0.08 g/dL. Mortality rate was significantly higher in patients with BAC≥0.08 g/dL. There was a significant difference in mechanism of injury based on BAC, which may have been attributed to mean age differences between groups. There were no differences in LOS, GCS, and ISS, though higher mortality in the BAC≥0.08 g/dL group may explain why no difference was observed in LOS. Assisted respiratory rate was significantly higher in the BAC<0.08 g/dL group. No difference was found in ethnicity distribution between the groups, though records were limited and require further investigation.

Conclusions: The results suggest that having a BAC≥0.08 g/dL in pediatric patients correlated with increased mortality rate and differences in mechanisms of injury, when compared to a BAC<0.08 g/dL. Consistent with existing literature, the data indicate that community-wide interventions should be implemented to educate on prevention, toxicity risks, and child supervision, minimizing risk of injury and mortality.

EFFICACY OF PHOTOPHERESIS IN PATIENTS WITH CHRONIC LEFT VENTRICULAR DYSFUNCTION

E. Chow, P. Deckerman, N. Satish, M. Lee, M. Hamilton, J. Kobashigawa
Cedars-Sinai Smidt Heart Institute, Los Angeles, California, UNITED STATES|

ABSTRACT BODY:

Purpose of Study: Photopheresis (ECP) is a therapeutic approach for modulating the immune system in heart transplantation (HTx). ECP has been used in patients (pts) with T cell mediated disease states (psoriasis) with success. ECP promotes expansion of regulatory T cells, suppressing pathogenic immune response driving disease process. Kirklin et al. provided evidence that supports ECP as a valuable treatment for rejection in HTx pts. We evaluated the efficacy of ECP in pts with chronic left ventricular dysfunction (LVD).

Methods Used: Between 2010 and 2024, we evaluated 16 HTx pts with chronic LVD referred for ECP, with history of left ventricular ejection fraction (LVEF) ≤ 40% due to recurrent rejection, including acute cellular rejection (ACR; n=5), biopsy-negative rejection (BNR; n=4), antibody-mediated rejection (AMR; n=5), or combined ACR/AMR (n=2). All received standardized 6-month ECP regimen (18 sessions). Cardiac function was assessed at baseline (biopsy), treatment end (6 mos), and 6 mos after completing ECP (12 months). Endpoints included: troponin, BNP, subsequent recurrent rejection within 1 year (yr), de novo donor specific antibodies (dnDSA), and 1-yr freedom from non-fatal major adverse cardiac events (NF-MACE).

Summary of Results: ECP was successful in 50% (n=8/16) of pts with LVD immediately post treatment and at 6 mos post-treatment; median time to ECP was 1.00 [0.83-1.40] yrs. Pts with ACR, 40% (n=2/5) maintained an LVEF ≥ 45% immediately post treatment, which improved to 60% (n=3/5) of pts at 6 mos post-treatment. Pts with AMR, 60% (n=3/5) showed immediate improvement post treatment, increasing to 80% (n=4/5) of pts at 6 mos post-treatment. Of pts with both ACR/AMR , none (n=0/2) demonstrated improvement LVEF ≥ 45% immediately post treatment, but 50% (n=1/2) showed LVEF improvement to ≥ 45% at 6 mos post-treatment. In the BNR group, 75% (n=3/4) showed improvement immediately post-treatment, but none (n=0/4) maintained improvement at 6 mos. BNP levels demonstrated a downward trend immediately post treatment for at least 6 mos. Freedom from subsequent rejection in 1 yr was 75% (12/16), and 81.25% (13/16) remained free of NF-MACE within 1-yr post-treatment. At the start of ECP, 18.75% (n=3/16) of pts had dnDSA. One pt (6.2%, n=1/16) developed dnDSA following ECP.

Conclusions: ECP appears to improve LVEF in pts with recurrent rejection and chronic LVD post treatment. ECP rates of improvement are more similar among pts with ACR or AMR than BNR. Larger studies are needed.

EFFECTIVENESS OF STATIN THERAPY FOR ELEVATED LIPID LEVELS IN PATIENTS ON MTOR INHIBITORS AFTER HEART TRANSPLANTATION

E. Chow, P. Deckerman, M. Lee, N. Satish, M. Hamilton, J. Kobashigawa.
Cedars-Sinai Smidt Heart Institute, Los Angeles, California, UNITED STATES|

ABSTRACT BODY:

Purpose of Study: Cardiac allograft vasculopathy (CAV) remains a major limiting factor for long-term survival following heart transplantation (HTx). Randomized control trials have demonstrated that one therapeutic strategy to slow the progression of CAV is the use of mTOR inhibitors (mTORi), including sirolimus and everolimus. However, a known side effect of mTORi is the elevation of lipid levels, particularly cholesterol, a well-established risk factor for CAV. Statin therapy, widely used for its lipid-lowering and immunomodulatory effects, has also been shown to reduce the development and progression of CAV. Yet, the efficacy of statins in managing hypercholesterolemia in HTx patients on mTORis remains unclear. Therefore, we aimed to evaluate the efficacy and safety of statin therapy in reducing lipid levels in HTx patients on mTORis.

Methods Used: Between 2010 to 2024, we assessed 41 HTx recipients who were transitioned from pravastatin, a low potency statin, to a high potency statin, specifically rosuvastatin or atorvastatin, after initiating mTORi therapy. Total cholesterol, HDL, LDL, and triglycerides, were evaluated at three time points: prior to mTORi initiation, prior to the switch to high potency statin, and approximately 12 months following statin intensification.

Summary of Results: Statin therapy resulted in a 23.3% reduction in total cholesterol levels in patients receiving mTORis. The median time to mTORi initiation after HTx was 374 days [301, 845] and the median time to statin initiation after mTORi initiation was 351 days [252, 439]. Of the 41 patients, 70.7% (n=29) received sirolimus and 29.3% (n=12) everolimus. Regarding statin choice, 78% (n=32) were switched to rosuvastatin 20 mg [Q1: 10 mg, Q3: 20 mg], while 22% (n=9) transitioned to atorvastatin 20 mg [Q1:10 mg, Q3:40 mg]. Following mTORi initiation, total cholesterol, LDL, and triglycerides increased significantly while HDL showed a modest but significant increase (see table 1). After switching to high potency statins, total cholesterol and LDL significantly decreased. Triglycerides trended, while HDL levels remained unchanged. Statin therapy was discontinued or dose-reduced due to intolerance in 5% (n=2/41) of patients within the 1-year study period.

Conclusions: Switching patients to high potency statin therapy effectively lowered lipid levels in heart transplant recipients on mTORis. Statin intensification (select dosing) appears safe and well tolerated in this population.

POSTER PRESENTATIONS

CARDIO-METH-ABOLIC SYNDROME: IMPACT OF CARDIAC COMORBIDITIES IN CONJUNCTION WITH METHAMPHETAMINE USE IN THE EMERGENCY DEPARTMENT AND STREET MEDICINE.

A. Narasimhan, K. Wieselthier, E.J. Lyon, G. Khatkar, S.A. Yip, Z.I. Hall, M. Menon, S. Fuchs.
College of Osteopathic Medicine of the Pacific, Western University of Health Sciences, Pomona, California, UNITED STATES|

ABSTRACT BODY:

Purpose of Study: Methamphetamine use is rising nationally, with certain regions and populations disproportionately affected. Methamphetamine-associated cardiomyopathy (MACM) is an emerging cause of emergency visits and hospitalizations, yet the role of coexisting conditions (hypertension, diabetes, chronic kidney disease, pulmonary disease, and obesity) remains unclear. This study examines the relationship between these comorbidities and MACM risk in acute care situations.

Methods Used: We conducted a retrospective analysis within our IRB-approved street medicine cohort which assesses the impact of methamphetamine route of administration on the severity and progression of heart failure. Comorbidities, including hypertension, diabetes mellitus, and congestive heart failure, were tallied descriptively to illustrate real-world burden. To contextualize our findings, we compared them with published literature describing comorbidities and their association with outcomes in MACM.

Summary of Results: In our street medicine MACM cohort (n=86), comorbidities were common: hypertension in 14 patients (16.3%), congestive heart failure in 10 (11.6%), and diabetes mellitus in 7 (8.1%), with many patients additionally having decreased left ventricular ejection fraction (LVEF). Published cohorts [SF1] show a similar pattern, with hypertension most prevalent (affecting >50% of patients). Among comorbidities, chronic kidney disease is the strongest predictor of adverse outcomes (OR ~5.5), followed by diabetes mellitus (OR ~3.0) and pulmonary disease (OR ~2.4), each associated with decreased LVEF, increased admissions and prolonged hospitalizations. These findings highlight the compounding effect of traditional cardiovascular comorbidities on MACM severity and acute care utilization.

Conclusions: MACM outcomes are influenced not only by methamphetamine use patterns and routes of administration but also by the burden of coexisting cardiovascular conditions. Hypertension is most prevalent, CKD the strongest predictor, while diabetes, pulmonary disease, and CHF add further risk. Our street medicine data underscore the need for systematic comorbidity screening in outreach populations. Integrating comorbidity burden into ED risk stratification and community care may reduce acute care utilization and improve long-term outcomes for vulnerable methamphetamine users at risk for MACM.

HYBRID METHACRYLATED GELATIN-HYALURONIC HYDROGELS FOR CARDIAC REGENERATION

A. Abou Jaoude, N. Najafi, E. Chen, F.G. Thankam.

Western University of Health Sciences College of Osteopathic Medicine of the Pacific, Pomona, California, UNITED STATES|

ABSTRACT BODY:

Purpose of Study: Myocardial infarction results in irreversible cardiomyocyte loss, scar formation, and progressive ventricular dysfunction. Injectable or implantable hydrogels capable of mimicking cardiac extracellular matrix (ECM), while offering electrical conductivity and water kinetics, may enhance regenerative repair. We aim to develop a blend of methacrylated gelatin (GHA) and methacrylated hyaluronic acid (HHA) hydrogels progressing cardiac tissue engineering.

Methods Used: GHA and HHA were synthesized via reaction with methacrylic anhydride, dialyzed, and lyophilized for storage. Hydrogels were fabricated at varying blend ratios 100:0, 75:25, 50:50, 25:75, 0:100 for GHA:HHA. The hydrogel precursor blends were photopolymerization with Irgacure combined with redox crosslinking of 2-hydroxy ethyl acrylate and acrylic acid. Conduction was assessed using dry hydrogels, phosphate-buffered saline (PBS), and water swollen hydrogels. Gravimetric analysis was used to analyze swelling kinetics at timed intervals for 60 minutes. Biodegradability was assessed by quantifying the alterations in dry weight and pH. Biocompatibility was tested with H9c2 cardiomyoblasts.

Summary of Results: HHA hydrogels in PBS exhibited reproducible electrical conductivity (average voltage 41.98 mV, resistance 0.636 MΩ, current 0.18 μA), while diH2O treatment increased resistivity (28.7 mV, 44.9 MΩ, 0.4 μA). GHA hydrogels demonstrated the highest conduction in PBS (74.2 mV, 203.2 MΩ, 0.5 μA). HGA hydrogels showed lower conduction but stable resistive properties (average 14.5 mV, 156.5 MΩ, 0.1 μA). Water swelling kinetics revealed gradual increase in water content across all formulations, with H100 and G100 demonstrating highest swelling capacity. Notably, G25H75 blends showed favorable handling with balanced swelling and conduction profiles, whereas G100 exhibited greater rigidity. H9c2 cultures demonstrated sustained viability and proliferation on all formulations.

Conclusions: Methacrylated GHA/HHA hydrogels exhibit hydration-driven conductivity, favorable swelling behavior, and biocompatibility, supporting their potential as scaffolds for cardiac tissue repair. Differential performance across formulations suggests that blend ratio tuning may optimize hydrogel for dynamic application in myocardial environments. These findings highlight the promise of hybrid biopolymer hydrogels for cardiac regeneration.

REPARATIVE RESPONSES OF TRANSFORMING GROWTH FACTOR-β1-POSITIVE EPICARDIAL ADIPOSE TISSUE-DERIVED STEM CELLS IN CARDIAC ISCHEMIA

S. Mukadam, D.S. Vayser, F.G. Thankam.

Western University of Health Sciences College of Osteopathic Medicine of the Pacific, Pomona, California, UNITED STATES|

ABSTRACT BODY:

Purpose of Study: Transforming growth factor-β1 (TGFβ1) is a central effector of post-infarct remodeling, driving fibroblast activation and cardiac extracellular matrix (ECM) deposition. TGFβ1 signaling is associated with early protective processes such as scarless healing and immunomodulation. Our group reported the communication between epicardial adipose tissue-derived stem cells (EATDS) and ischemic myocardium, suggesting their critical role in responding to myocardial pathology. EATDS represent a heterogeneous population spanning from regenerative to pathological phenotypes. As an indicator of cardiac repair, we hypothesize that the status of TGFβ1 in EATDS represents regenerative phenotypes. This study aimed to assess the status of TGFβ1 in ischemic EATDS and define the phenotypic subsets based on signature genes and associated pathways at single-cell resolution.

Methods Used: EATDS were isolated from swine myocardium, characterized in culture, and subjected to in-vitro ischemia and reperfusion. TGFβ1 expression was quantified using RT-qPCR, immunofluorescence, and Western blot. A single-cell RNA sequencing data repository was established and TGFβ1+EATDS were screened. Gene enrichment analysis of key signature genes displayed by the subpopulation identified that the major pathways involved were related to fibrosis and repair.

Summary of Results: EATDS exhibited ischemia tolerance. TGFβ1 was higher in the ischemia and reperfusion groups at transcript and protein levels relative to control; however, the transcript-level increase was statistically not significant. Single-cell profiling revealed TGFβ1+EATDS proliferating subsets in reperfusion, with transcriptional reprogramming toward nucleotide biosynthesis and regenerative transcripts such as ALDH1A1. Additionally, TGFβ1+ EATDS stromal subsets exhibited ischemia-induced upregulation of SELENBP1, indicating redox adaptation. Pathway analysis identified immunoregulatory signaling and ECM remodeling, linking TGFβ1+EATDS to reparative processes.

Conclusions: TGFβ1 is a persistent yet heterogeneous regulator of EATDS responses to ischemia-reperfusion. Proliferating subsets engaged fibrogenic programs, fibroblast pools displayed contractile phenotypes, and stromal cells activated oxidative pathways, reflecting a balance between repair and maladaptation. By defining gene signatures and pathways in TGFβ1+EATDS, the findings propose potential applications in cell-based therapies; however, further investigations are warranted to extrapolate these findings to the clinical arena.

LONGITUDINAL GROWTH ANALYSIS OF NASAL SEPTAL DEVIATION AND SINUS DEVELOPMENT DURING CRANIOFACIAL GROWTH

A. Hardin[1], M. Pirodan[2], S.F. Zaidi[2], M. Boparai[2], C. Mercado[2], A. Wyckoff[2].

[1]Western University of Health Sciences College of Osteopathic Medicine of the Pacific-Northwest, Lebanon, Oregon, UNITED STATES|

[2]Western University of Health Sciences College of Osteopathic Medicine of the Pacific-Northwest, Lebanon, Oregon, UNITED STATES|

ABSTRACT BODY:

Purpose of Study: The study aims to determine whether longitudinal changes in nasal septal deviation (NSD) during craniofacial growth are associated with paranasal sinus development and to assess their implications for pediatric airway obstruction. By examining radiographic data from patients aged 8 to 18 years, this study aims to evaluate NSD across critical developmental stages of facial growth. In contrast to previous studies that have largely evaluated septal deviation in isolation or in adult populations, this study investigates the developmental interplay between septal alignment and paranasal sinus growth across childhood and adolescence. Establishing these relationships may clarify whether NSD is primarily a consequence of normal growth processes, pathological influences, or a combination of both, thereby contributing to a deeper understanding of the structural basis for airway obstruction which may inform indications for clinical approaches to pediatric and adolescent populations.

Methods Used: This study analyzed antero-posterior and lateral cephalographs from 27 individuals (9 females, 18 males) in the Bolton Brush longitudinal growth study, with paired radiographs at ages 9 and 18 years. Five researchers established a standardized landmarking protocol in 3D Slicer, placing points along the nasal septum, nasal cavity, and maxillary and frontal sinuses. Measurements included percentage septal deviation and sinus dimensions (antero-posterior length, supero-inferior height). Linear models assessed associations of septal deviation with sex, sinus size, and changes across growth.

Summary of Results: No significant associations were found between nasal septal deviation and sex, maxillary sinus size, or frontal sinus size at either 9 or 18 years of age. Similarly, proportional changes in sinus dimensions did not correspond with changes in septal deviation.

Conclusions: Nasal septal deviation appears to develop largely independently of sinus growth and sex differences, suggesting other influences such as localized asymmetry, genetic factors, or pathology. Despite the limitations of two-dimensional radiographs, this longitudinal study highlights developmental trends in NSD. Future research using CT and advanced 3D morphometric techniques, such as Spherical Harmonics (SPHARM), may clarify underlying mechanisms and clinical implications for pediatric airway obstruction.

CARDIAC STROMAL CELL REPAIR RESPONSES MEDIATED BY ISCHEMIA-INDUCED METABOLITES

E. Rostomian, A. Postajian, F.G. Thankam.

College of Osteopathic Medicine, Western University of Health Sciences, Pomona, California, UNITED STATES|

ABSTRACT BODY:

Purpose of Study: Ischemic heart disease is a leading cause of morbidity and mortality, owing to the limited regenerative potential of the myocardium. Stromal cells within the myocardium (LVSCs) and epicardial adipose tissue (EATDS) are non-myocyte populations activated by ischemic stress that influence repair through metabolite-driven paracrine signaling. We hypothesized that metabolites released by LVSCs and EATDS under ischemia promote survival and reparative responses. The goal was to identify ischemia-induced metabolites and assess their effects on repair-associated gene programs.

Methods Used: LVSCs and EATDS were subjected to ischemic challenge in vitro. Metabolomic profiling EATDS and LVSCs was performed using liquid chromatography-mass spectrometry (LC-MS) following standard metabolite extraction protocols and analyzed using LC-MS to generate raw spectral data. The acquired spectra were processed using MAVEN software for peak detection, alignment, and quantification. LVSCs and EATDS were treated with candidate metabolites (sarcosine, 3-hydroxypropanoic acid, and 2-pyrrolidone-5-carboxylic acid) under ischemic conditions to assess their survival. Expression of cardiac repair-associated markers (GATA4, NKX2.5, TBX5, IRX4, TROP, LGAL1, CXN43) was evaluated using qRT-PCR.

Summary of Results: Metabolomic profiling of EATDS revealed the differential screening of 68 metabolites whereas LVSCs displayed 65 compounds. Three candidate metabolites enriched during ischemia in both the cells were: sarcosine, 3-hydroxypropanoic acid, and 2-pyrrolidone-5-carboxylic acid. Among these, sarcosine demonstrated the strongest pro-reparative effect. In LVSCs, sarcosine markedly upregulated transcription factors (GATA4, NKX2.5, TBX5, IRX4) and structural/functional proteins (TROP, LGAL1, CXN43). EATDS exhibited modest upregulation of the transcription factors under sarcosine treatment, while the other metabolites elicited only basal expression of reparative markers.

Conclusions: Ischemia-induced metabolites reflect the pathological/physiological status of cardiac stromal cells. Sarcosine activates transcriptional and structural programs linked to regeneration, highlighting its role in myocardial repair. These findings elucidate the importance of metabolic crosstalk between stromal populations in the ischemic heart that could benefit cardiac recovery.

ACUTE HEMOTHORAX FOLLOWING TUNNEL DIALYSIS CATHETER PLACEMENT

N.E. Salm[1], A. Garrison[1], D. Damron[1], J. Holland[2], M. Zia[3].

[1]Western University of Health Sciences College of Osteopathic Medicine of the Pacific-Northwest, Lebanon, Oregon, UNITED STATES|

[2]Department of Anesthesiology, University of Missouri-Kansas City School of Medicine, Kansas City, Missouri, UNITED STATES|

[3]Department of Internal Medicine, University of Missouri-Kansas City, Kansas City, Missouri, UNITED STATES|

ABSTRACT BODY:

Case Report: Tunneled dialysis catheters (TDCs) are commonly used in hemodialysis to provide stable, recurrent vascular access. This is achieved by accessing the right internal jugular vein (IJV) and advancing it into the superior vena cava, positioning the tip near the right atrium. An anterior-posterior (AP) chest x-ray is routinely utilized to confirm proper catheter placement (1) and evaluate for potential complications such as hemorrhage, venous thrombosis, venous occlusion, or catheter misplacement (2). We present the case of a 47-year-old female, BMI 25, who underwent routine TDC placement into her right IJV for intermittent hemodialysis pending AV fistula maturation. The procedure was uncomplicated, with the wire and catheter advanced under fluoroscopy without resistance. Aspiration and flushing confirmed patency intraoperatively. An immediate post-procedure AP chest radiograph showed no evidence of pneumothorax; however, Radiology later reported acute progression of preexisting right lung pleural-parenchymal disease. Within an hour post-procedure, the patient developed acute dyspnea, diaphoresis, and a sense of impending doom, with rapid progression to cardiac arrest. Return of spontaneous circulation (ROSC) was achieved following prolonged resuscitation efforts and placement of two chest tubes, with approximately 1 liter of sanguineous output. Subsequent imaging revealed the TDC transecting through the azygos vein, with active extravasation into the right pleural space. To control hemorrhage, the catheter was left in situ as a tamponade to prevent further expansion of the hemothorax. While aberrant placement is rare, central vein perforation is a critical procedure ocedural complication. This case highlights the need to maintain intravascular perforation as a differential diagnosis in post-procedural deterioration, even after technically smooth TDC placement. Incorporating lateral imaging, in addition to standard AP radiographs, may facilitate the early detection of malposition and help prevent severe complications.

MISOPROSTOL FOR POSTPARTUM HEMORRHAGE IN SOUTH ASIA: BARRIERS AND SOLUTIONS IDENTIFIED BY LITERATURE REVIEW

A. Swarna[1], S. Tamatam[1], T. Chowdhury[1], I. Deshpande[1], H. Vendidandi[2], A. Nelson[1].

[1]College of Osteopathic Medicine of the Pacific, Western University of Health Sciences, Pomona, California, UNITED STATES|

[2]Touro University California, Vallejo, California, UNITED STATES|

ABSTRACT BODY:

Purpose of Study: We investigated reasons for misoprostol underutilization as a safe option for postpartum hemorrhage (PPH) prevention in South Asia, as the WHO reported in 2024 that this region, combined with Sub-Saharan Africa, had the highest prevalence of maternal deaths from PPH around the world (>80%). Using this drug to prevent PPH in these countries seems to be under researched, so we searched peer-reviewed articles to provide more information regarding the unique challenges that exist here.

Methods Used: We conducted a narrative review of English language peer-reviewed articles published between January 1, 2004 and January 1, 2024 and listed on PubMed, Embase, and Google Scholar using search words “misoprostol”, “postpartum hemorrhage”, and South Asian country names. Articles were included if they reported barriers to misoprostol use for PPH in these countries based on randomized controlled trials, observational designs, or population-based surveys or if they addressed the demonstrated barriers. A thematic analysis was performed to identify common barriers.

Summary of Results: We identified 1960 papers; 15 met inclusion criteria. Two barriers were identified. Firstly, two thirds of papers reported that lack of community-based distribution systems was a barrier. Successful models included using trained community health workers (CHWs) or paramedics to distribute the drug. Compared to other regions of the world, such as the United States, there is a stronger need for efficient distribution, considering Sushmita Das *et al.* (2016) reported that as many as 70% of women in South Asian deliver at home. Second, one third of articles cited limited drug availability, often due to stockouts and limited local manufacturers. The cost-effectiveness of using misoprostol was frequently mentioned, especially for home births.

Conclusions: Due to its various advantageous properties, such as heat stability, easy administration, and potency, misoprostol has great life-saving potential; however widespread lack of access was universally reported. Utilizing CHWs might improve distribution, but drug shortages remain. In these resource-poor countries, maternal morbidity from PPH needs higher priority and policy makers must look beyond its use in medicated abortion to appreciate misoprostol’s lifesaving potentials later in pregnancy. Once more research is conducted to address these barriers, policy reform and local manufacturing investments should occur to reduce maternal mortality.

SUNKEN FLAP SYNDROME IN ACUTE REHABILITATION: A CASE OF POSITIONAL NEUROLOGICAL DECLINE IMPROVED BY SHUNT ADJUSTMENT

C. Tong[1], J. Tram[2], A. Pham[2], R. Romeu[3].

[1]College of Osteopathic Medicine of the Pacific, Western University of Health Sciences, Pomona, California, UNITED STATES|

[2]Physical Medicine and Rehab, University of California Los Angeles David Geffen School of Medicine, Los Angeles, California, UNITED STATES|

[3]TBI, Ranchos Los Amigos, Downey, California, UNITED STATES|

ABSTRACT BODY:

Case Report: Sunken Flap Syndrome is a rare complication following decompressive craniectomy, marked by visible scalp depression with new or worsening neurological symptoms. It usually develops weeks to months postoperatively when atmospheric pressure exceeds intracranial pressure, displacing skin and brain tissue. This can cause cognitive decline, altered mental status, or paradoxical herniation. Symptoms often improve after cranioplasty, which restores normal intracranial pressure. Early recognition is essential to prevent lasting deficits. This case describes a 35-year-old male presented after assault with a ruptured A2 aneurysm, left frontal intraparenchymal and subarachnoid hemorrhages, and multiple subdural hematomas. He underwent right hemicraniectomy with external ventricular drain placement, later requiring left external ventricular drain (EVD) replacement and ventriculoperitoneal (VP) shunt insertion with drainage setting at Certas 7. After stabilization, he was discharged to acute rehab. Throughout acute rehab, he presented with somnolence, disorientation, postural headaches, and fluctuating left upper extremity weakness (5/5 to 2/5). Symptoms drastically improved with Trendelenburg positioning and IV fluids, however interventions had temporary effects with symptoms returning within hours. CT Head later showed leftward midline shift, sunken scalp flap, uncal herniation, and decreased ventricular size. Adjustment of VP shunt to Certas 8 led to near-complete resolution, allowing the patient to tolerate upright positioning and participate in therapies. In rehabilitation, distinguishing hydrocephalus, post-traumatic headache, and sunken flap syndrome is critical.

Hydrocephalus typically presents with ventriculomegaly and improves after CSF diversion. Migrainous headaches are usually non-positional and lack acute neurological decline. By contrast, sunken flap syndrome is characterized by positional neurological deterioration, improvement with Trendelenburg or IV fluids, and visible scalp concavity. CT imaging helps differentiate these conditions and guides shunt management. Risk factors for sunken flap syndrome include large craniectomy defects, delayed cranioplasty, CSF drainage, and severe TBI. Conservative measures such as fluids and postural adjustments may provide temporary stabilization, but definitive treatment requires cranioplasty, which restores intracranial pressure dynamics and improves functional recovery.

UNDERSTANDING DERMATOLOGICAL HEALTH: KNOWLEDGE OF COMMON SKIN CONDITIONS IN OLDER ADULTS

K. Parnala, A. Felty, M. Steinauer.
Western University of Health Sciences, Pomona, California, UNITED STATES|

ABSTRACT BODY:

Purpose of Study: The goal of this project is to increase awareness and understanding of common skin conditions in older adults, with a focus on prevention, early detection, and effective management. By educating participants, the project aims to promote proactive skin health practices and enhance overall well-being among older adults. Specifically, it seeks to identify prevalent benign skin conditions and various types of skin cancer while helping individuals recognize early warning signs that may indicate the need for medical attention. Additionally, it will provide practical strategies for maintaining healthy skin, and encourage timely medical evaluation by increasing awareness of when to seek professional care. This approach aims to reduce complications that can arise from delayed treatment.

Methods Used: This study employs a mixed-methods design consisting of both quantitative and qualitative elements. The quantitative component includes a post-presentation survey utilizing a Likert scale and multiple-choice questions to assess participants' knowledge, confidence, and behavioral intentions related to skin health. The qualitative component comprises open-ended questions that capture participants' feedback on the presentation and areas of interest for future education.

Summary of Results: Five participants completed the post-presentation survey following the educational session at the Lebanon Senior Center. While the small sample size limits statistical analysis, preliminary findings suggest trends toward increased confidence and awareness in recognizing and managing common skin conditions. Participants reported greater understanding of age-related skin changes, preventive strategies such as sun protection, moisturization, and the importance of performing self-examinations. Open-ended responses highlighted appreciation for practical tips and resources, including the distribution of sunscreen samples and informational handouts.

Conclusions: Although the limited number of responses restricts the generalizability of these findings, this pilot project demonstrates the feasibility of delivering targeted dermatological health education to older adults in community settings. The project underscores the need for expanded data collection to assess outcomes more robustly and supports the integration of skin health education into preventive care for aging populations.

ASSOCIATION OF LOW-DENSITY LIPOPROTEINS AND TENDON DEGENERATION IN SHOULDER TENOCYTES

K. Vartanian[1,2], E. Rostomian[1,2], J. Anderson Enni[1,2], F.G. Thankam[1,2],
[1]Translational Research, Western University of Health Sciences, Pomona, California, UNITED STATES|
[2]Western University of Health Sciences, Pomona, California, UNITED STATES|

ABSTRACT BODY:

Purpose of Study: Shoulder tendon injuries (STIs) are a leading cause of musculoskeletal disability, often resulting in chronic pain, impaired mobility, and invasive surgical intervention. Current treatments carry significant risks and variable outcomes, highlighting the need for targeted approaches. Hyperlipidemia, especially increased low-density lipoprotein (LDL), has been associated with tendon degeneration by promoting oxidative stress, inflammation, and extracellular matrix (ECM) disruption. Yet, the direct impact of LDL on shoulder tenocytes remains poorly defined. We propose that LDL exposure alters the expression status of tendon homeostasis genes leading to degenerative changes.

Methods Used: Shoulder tenocytes and LDL were isolated from Yucatan swine and cultured in LDL-supplemented media. Viability was assessed by MTT assay, cell morphometry by phase-contrast microscopy, and biomarker expression by qRT-PCR, immunofluorescence, and Western blotting. Markers included COL-I, COL-III, SCX, PLIN2, VIM, ATP5A, TFAM, and TNMD.

Summary of Results: Swine LDL was isolated by density-gradient ultracentrifugation and validated by SDS-PAGE analysis revealing the intense band above 250kDa. A progressive decline in tenocyte viability was observed in a concentration dependent manner upon LDL exposure. LDL-exposed tenocytes displayed altered tenocyte morphometry characterized by increased granularity and circularity compared to the control. Also, alteration in the expression status of COL-I, COL-III, SCX, PLIN2, VIM, ATP5A, TFAM, and TNMD were observed in LDL-exposed tenocytes.

Conclusions: LDL impacts shoulder tenocyte homeostasis, implicating hyperlipidemia as a molecular driver of tendon degeneration. Moreover, LDL exposure alters the expression of tendon homeostasis genes, thereby accelerating the pathological response. Further understanding regarding the underlying molecular mechanisms could support the development of effective strategies addressing STI.

REDHEAD RESISTANCE: ANESTHETIC TOLERANCE WITH MELANOCORTIN-1 RECEPTOR LOSS OF FUNCTION MUTATIONS

L. Bates[1], S. Fuchs[2].

[1]Western University of Health Sciences College of Osteopathic Medicine of the Pacific-Northwest, Lebanon, Oregon, UNITED STATES|

[2]Western University of Health Science, College of Osteopathic Medicine of the Pacific, Pomona, California, UNITED STATES|

ABSTRACT BODY:

Purpose of Study: The conversation around redheads needing more anesthesia continues to be controversial and divisive amongst practicing anesthesiologists. For years, the natural pigmentation of a patient's hair and tone of their skin has been a debated pre-operative check among anesthesiologists due to the thought that red-headed patients require more anesthesia to achieve general anesthesia. This project aims to identify in the published literature if a link could be established between the genes and proteins associated with the redhead skin tones and such pathways involved in the mechanism of action of anesthetic drugs.

Methods Used: This review started with investigation into eighteen articles to evaluate the functionality of MC1R mutations and how they are represented in anesthesia studies. Through systematic review using the following keywords: anesthesia, melanocortin-1 receptor, red hair, genetics, mechanisms, tolerance, and nociception. Fifteen studies in the last 25 years were selected and sorted into "Fact" or "Myth" depending on the outcome of the study. Four papers were excluded for not containing original research.

Summary of Results: Through experimentation on mice and humans, it was determined that those with natural red hair and loss of MC1R function did have elevated basal pain thresholds due to decreased melanocytic proopiomelanocortin transcription and systemic melanocyte-stimulating hormone (MSH) levels in the plasma of redhaired mice. Decreased peripheral α-MSH derepresses the central opioid tone mediated by the opioid receptor OPRM1, resulting in increased nociceptive thresholds. Seven studies provided evidence that MC1R mutations do increase anesthesia requirements for local and inhaled anesthetics while four studies argued against. Mechanism for interaction is widely unknown but has been theorized to have a relationship to inflammatory factors, nitric oxide, or protein kinases. The data mentions confounding variables of weight, ASA status, and sex that can also contribute t changes in anesthesia requirements. The proposed mechanism of action involves nitric oxide reduction and decreased peripheral MSH but the interaction with anesthetics is unclear in current research.

Conclusions: Overall, patients with homozygous MC1R mutations should be questioned as if they will respond poorly to anesthetics to avoid awareness or unnecessary pain. Future studies should investigate the mechanism as to how MC1R functionality impacts the effectiveness of anesthetics.

IMPACT OF NERVE BLOCK TIMING ON POST-OPERATIVE PAIN AND OPIOID USE IN TOTAL KNEE ARTHROPLASTY PATIENTS

A. Garrison[1], N.E. Salm[1], D. Damron[2], J. Holland[3], K. Jezierski[3].

[1]Western University of Health Sciences College of Osteopathic Medicine of the Pacific-Northwest, Lebanon, Oregon, UNITED STATES|

[2]Western University of Health Sciences, Pomona, California, UNITED STATES|

[3]Anesthesiology, University of Missouri- Kansas City, Kansas City, Missouri, UNITED STATES|

ABSTRACT BODY:

Purpose of Study: Regional anesthesia has become one of the primary methods for post-operative pain management in patients undergoing total knee arthroplasty (TKA), resulting in decreased post-operative opioid use, length of stay (LOS), and improved patient satisfaction scores. Kim et al. (2019) found that patients receiving preoperative femoral and sciatic nerve blocks reported significantly lower pain scores in the first 18 hours postoperatively compared to those who did not. Multiple societies, including the American Society of Regional Anesthesia and Pain Management (ASRA), recommend peripheral nerve blocks (PNBs) such as the lateral popliteal, IPACK, sciatic, femoral, and adductor canal block, which are integral to Enhanced Recovery After Surgery (ERAS) protocols. Prior studies have largely focused on comparing PNB types, such as Jaremko *et al.* (2021), who found lower opioid requirements with distal femoral triangle and adductor canal blocks compared to femoral blocks alone.

Methods Used: We retrospectively identified 600 adult patients who underwent primary TKA using spinal anesthesia from 1/1/2020-1/1/2025, who also received a pre-operative or post-operative adductor canal PNB. The primary outcome was the total morphine milligram equivalents (MME) consumed within 48 hours postoperatively, with secondary outcomes including MME at 24 hours and LOS. The mean MME and standard deviation were calculated for each group and analyzed using an independent t-test.

Summary of Results: Preliminary data revealed that 414 patients who received preoperative adductor canal PNBs consumed 71.5 MME ± 25.4 MME and 126.4 ± 35.7 MME at 24 and 48 hours, respectively. In contrast, 186 patients with postoperative PNBs consumed 132 ± 51.3 MME and 193.9 ± 70.5 MME, respectively. Statistical analysis showed pre-operative adductor canal PNBs had decreased MME requirements at 24 hours (t-test 2.3616, $p = 0.0458$), while MME requirements at 48 hours show that post-operative blocks are non-inferior to pre-operative blocks.

Conclusions: Our preliminary findings suggest that pre-operative adductor canal PNBs have decreased MME requirements in the first 24 hours post-operatively, with no statistically significant difference in MME requirements at 48 hours or LOS. Further data collection and analysis are warranted to assess for statistical differences in MME requirements at 48 hours, reported pain scores, and variations in type, concentration, and volume of local anesthetic used for adductor canal PNBs.

HIGH-DOSE SIMVASTATIN AS A POTENTIAL TRIGGER FOR ANGIOEDEMA: A CASE REPORT FOR BROADER DIAGNOSTIC CONSIDERATION

J. Lacsamana[1], B. Han[1], M. Han[2], S.W. White[3].

[1]Western University of Health Sciences College of Osteopathic Medicine of the Pacific, Pomona, California, UNITED STATES|

[2]The University of Texas at Austin Dell Medical School, Austin, Texas, UNITED STATES|

[3]Clinical Education, Western University of Health Sciences, Pomona, California, UNITED STATES|

ABSTRACT BODY:

Case Report: Angioedema is a potentially life-threatening condition involving swelling under the skin. The most common pharmacologic cause of this reaction is angiotensin-converting enzyme (ACE) inhibitor therapy, but other medications may contribute to the development of angioedema. This case describes a 68-year-old male who presented to the emergency department with tongue and lip swelling and was diagnosed with angioedema, initially attributed to lisinopril use. However, outpatient follow-up revealed that the only recent medication change was an inadvertent supratherapeutic 60 mg daily dose of simvastatin. Furthermore, the patient was found to have a medical history of angioedema secondary to atorvastatin use. Based on his history, the ACE inhibitor was discontinued, and the statin dosage was reduced with symptom resolution. The patient's clinical course adds to the limited literature on statin-induced angioedema, particularly in the setting of concurrent ACE inhibitor use. It also underscores the importance of thorough medication reconciliation and avoiding premature diagnoses of the most common etiology.

THYROID MEDICATION ERRORS REPORTED TO THE UNITED STATES POISON CENTERS, 2000-2024

M. Lu[1], H. Hays[2], J. Badeti[2], N. Rine[2], M. Zhu[2], J. Yang[2], G. Smith[2].

[1]Western University of Health Sciences, Pomona, California, UNITED STATES|

[2]Center for Injury Research and Policy of Abigail Wexner Research Institute at Nationwide Children's Hospital, Columbus, Ohio, UNITED STATES|

ABSTRACT BODY:

Purpose of Study: To investigate the characteristics and trends of single-substance thyroid medication-related therapeutic errors that occurred in out-of-hospital settings reported to United States poison centers from 2000 to 2024.

Methods Used: National Poison Data System (NPDS) data were retrospectively analyzed. US population-based rates were calculated, and trends were analyzed.

Summary of Results: There were 89,614 reported thyroid medication therapeutic error-related exposures in nonhealthcare facility settings from January 1, 2000, to December 31, 2024, of which, 94.9% involved medications used to treat hypothyroidism (n=85,030) and 5.1% used to treat hyperthyroidism (n=4,584). The number of therapeutic errors increased by 337.1% during the study period. Although most therapeutic errors were clinically inconsequential, 67 hypothyroidism and 5 hyperthyroidism medication-related therapeutic errors resulted in critical care unit admissions, and 11 hypothyroidism and 1 hyperthyroidism medication-related therapeutic errors resulted in major effects. No deaths were reported. Females accounted for 77.2% of hypothyroid medication-related cases, and 71.2% involved adults 40 years and older. Likewise, females accounted for 75.6% of hyperthyroid medication-related cases, and 64.0% involved adults 40 years and older. Levothyroxin was the most common hypothyroidism medication reported (86.7%), although Liothyronine was almost 10 times more likely to be associated with a critical care unit admission (OR: 9.89, 95% CI: 4.25-23.0) and more than 40 times more likely to result in a major effect (OR: 40.59, 95% CI: 10.48-157.25) than other hypothyroidism medications combined. Methimazole was the most common hyperthyroidism medication reported (91.5%).

Conclusions: Serious consequences associated with thyroid medication-related therapeutic errors were uncommon, which supports the safety of these medications.

BASAL CELL CARCINOMA OF THE PERIANAL REGION TREATED WITH MOHS SURGERY: A CASE REPORT

R. Van Dyke[1], J. Saile, Surgery[2], K. Bickle[3].

[1]Western University of Health Sciences College of Osteopathic Medicine of the Pacific, Pomona, California, UNITED STATES|

[2]Keck Medicine of USC, Los Angeles, California, UNITED STATES|

[3]Newport Skin Cancer Center, Newport, California, UNITED STATES|

ABSTRACT BODY:

Case Report: Basal cell carcinoma [BCC] is the most commonly diagnosed cutaneous malignancy and typically arises in sun-exposed regions, such as the head and neck. It is exceedingly rare to develop BCC in the anogenital region, accounting for only 0.2% of reported cases. More often, lesions in the anogenital region are attributed to alternative etiologies, such as verruca vulgaris, dermatitis, or hemorrhoids, and may therefore be overlooked or minimized on physical exam. This report aims to highlight the importance of considering BCC as a differential diagnosis for suspicious anogenital skin lesions and discusses the recommended treatment approach.

This case report presents a 49-year-old female patient who presented to her gynecologist for routine evaluation and was found to have an asymptomatic perianal skin lesion on exam. Biopsy of the lesion revealed nodulo-infiltrative basal cell carcinoma, an aggressive form of BCC. The patient was referred to a dermatologic surgeon and subsequently underwent Mohs micrographic surgery for curative treatment without complications. The tumor required three stages to clear, and there was no indication of recurrence at the three-month mark. Although rare, basal cell carcinoma can arise in non-sun-exposed skin regions. As such, BCC should be included in the differential diagnosis for any suspicious perianal or genital lesions and tangential or excisional biopsy is recommended. Given the potential for locoregional damage, surgical resection, preferably with Mohs micrographic surgery, is the treatment of choice for BCC in the anogenital region to achieve the highest cure rate and preservation of healthy tissue.

NOVEL NANOPARTICLE-BASED DELIVERY OF CARVEDILOL FOR PREVENTING UV-INDUCED SKIN INFLAMMATION

T.J. Chu[1,2], A. Shahid[1], P. Desai[1], Y. Huang[1], T.J. Chu,[2].

[1]Western University of Health Sciences College of Pharmacy, Pomona, California, UNITED STATES|

[2]Western University of Health Sciences College of Osteopathic Medicine of the Pacific, Pomona, California, UNITED STATES|

ABSTRACT BODY:

Purpose of Study: Dysregulation of cytoplasmic calcium (Ca2+) level is a key mechanism in UV-induced skin inflammation and cancer. Our previous studies show that ryanodine receptors (RyRs), a family of Ca2+ channels located on the endoplasmic reticulum, are upregulated by UV radiation, leading to increased cytosolic Ca2+ release. Carvedilol, a clinically available β-blocker that antagonizes RyR activation, may be repurposed as a skin cancer preventive agent, though its current oral use is limited by poor solubility and bioavailability. Using nanotechnology, we set out to develop a novel formulation to improve carvedilol delivery and efficacy for cancer prevention.

Methods Used: 1) Carvedilol-loaded niosomes were prepared using the thin film hydration method. Predetermined ratios of Span80:Brij S20 (1:1) and cholesterol:carvedilol (4:1) were dissolved in chloroform:methanol (2:1, v/v) and optimized for particle size, polydispersity index (PDI), and zeta potential. Three critical conditions were examined: evaporation pressure, hydration temperature, and sonication time.

2) Twenty SKH-1 hairless mice were divided into four groups and administered treatment through drinking water: control, niosomal carvedilol (20 mg/kg), plain niosomes, and free carvedilol (20 mg/kg). Water consumption and body weight will be measured every other day. After 7 days of treatment, the mice will be exposed to a single dose of UV radiation (224 mJ/cm2) on the dorsal skin within a custom-designed UV exposure chamber. At 6 hours post-UV, mice will be euthanized and plasma levels of interleukin-6 (IL-6) measured by ELISA, as our prior work demonstrated IL-6 elevation following UV exposure.

Summary of Results: The optimized formulation was prepared by dissolving surfactants and carvedilol in a round bottom flask, followed by evaporation in a rotavapor under 350 mbar at 45°C for 1 hour to form a thin film. The resultant film was hydrated with 20 mL of PBS prewarmed to 50°C in an ultrasonic bath for 1 hour and equilibrated at room temperature for 15 minutes before characterization. Optimized carvedilol-loaded niosomes averaged particle size 232.2±129.5 nm, PDI 0.24±0.05, and zeta potential 2.5±11.8 mV. Animal studies are ongoing to evaluate the efficacy of oral niosomal carvedilol compared with free carvedilol on UV-induced IL-6.

Conclusions: Niosome-encapsulated carvedilol shows potential as a repurposed agent for preventing UV-induced skin damage, inflammation, and cancer.

EWING'S SARCOMA DOESN'T STOP AT AMPUTATION: RECURRENT CALCANEAL EWING'S SARCOMA WITH TIBIAL INVOLVEMENT IN AN ADOLESCENT

V.J. Gujrathi[1], R. Kukunoor[2].

[1]Osteopathic Medicine, Western University of Health Sciences, Pomona, California, UNITED STATES|

[2]Ironwood Cancer and Research Centers, Scottsdale, Arizona, UNITED STATES|

ABSTRACT BODY:

Case Report: Ewing's sarcoma is a highly aggressive malignant tumor that arises from primitive neuroectodermal cells and primarily affects bones. It most frequently occurs in adolescents and young adults, with a slight male predominance. Although long bones and the pelvis are the most common sites of involvement, Ewing's sarcoma can originate in the small hand and foot bones. These make up 3%-5% of reported cases and present with their own diagnostic and therapeutic challenges. We present the case of a 16-year-old male diagnosed with Ewing's sarcoma originating in the right calcaneus. Imaging done alongside chemotherapy after initial diagnosis revealed local metastasis to one of the adjacent cuneiform bones, but no evidence of distant metastatic spread. The patient underwent three months of induction chemotherapy consisting of ifosfamide, doxorubicin, and vincristine, resulting in a partial response. A below knee amputation was performed to achieve local control, followed by six months of adjuvant chemotherapy. Despite this aggressive multimodal approach, the patient experienced a local recurrence in the proximal tibia within the same extremity two years into remission from first occurrence. Biopsy of this recurrent lesion showed mutations in tumor suppressor SMARCA4. There is little data regarding recurrence of Ewing's post amputation specifically, but there is evidence that in roughly 5.2% of cases of osteosarcoma treated with amputation for local disease control, there will be a local recurrence at the amputation site. The tibial recurrence was treated with cyclophosphamide and irinotecan with radiation therapy for local control. Currently, the patient has been disease free for 52 months. This case highlights a unique presentation of Ewing's, the tumor's aggressive nature, the potential for disease persistence even after apparent initial control. It also demonstrates the importance of long-term surveillance. It raises considerations regarding tumor biology, possible micrometastatic disease at presentation, and the role of intensified or alternative therapeutic strategies for high-risk cases. This case aims to raise awareness for the need of continued research into prognostic factors and add to the limited existing literature on such cases. Cases like these may aid in the development of novel treatment approaches such as gene therapy or immunotherapy to improve outcomes in patients with rare and aggressive presentations of Ewing's sarcoma.

TRANSLATING ANTEROLATERAL LIGAMENT DISSECTION TO MEDICAL EDUCATION: A PRESERVED CADAVER APPROACH

K. Ngo[1], J. Atterholt[1], J. Son[2].

[1]Western University of Health Sciences College of Osteopathic Medicine of the Pacific, Pomona, California, UNITED STATES|

[2]Western University of Health Sciences College of Podiatric Medicine, Pomona, California, UNITED STATES|

ABSTRACT BODY:

Purpose of Study: Originally described by Paul Segond in 1879, the anterolateral ligament (ALL) has regained attention following its formal anatomical characterization in 2013. Subsequent studies have explored its role in rotational knee stability and its potential surgical relevance in anterior cruciate ligament reconstruction. Despite this, few educational dissection protocols exist to reliably dissect and identify the ALL on embalmed cadavers, particularly within medical school anatomy curricula. This study aims to develop and pilot reproducible, student-friendly dissection instructions for finding the ALL, building upon established procedures and adapting them for implementation at the first-year medical student level.

Methods Used: Knees of 12 embalmed donor patients from the WesternU Body Donation Program were utilized across 2 dissection trials. In the initial validation phase, we dissected 9 specimens to standardize an adapted protocol suitable for preserved donors. In the second phase, 6 first-year medical students working on 3 donors were randomly selected and assigned to dissect the ALL following the new protocol, which was implemented in formal curriculum on a trial basis to evaluate the efficacy of the protocol in an early learner context.

Summary of Results: In the validation phase, the ALL was successfully dissected and identified in 9/9 specimens (100%). In the pilot implementation phase, 1 of 3 first-year student groups was able to successfully identify the ALL using the guide. Common challenges included difficulty in distinguishing the ALL from adjacent fascia, adipose, and other ligamentous tissues in formalin-preserved specimens, as well as anatomical distortion caused by prior student dissections that occasionally disrupted or removed surrounding muscular and ligamentous structures. Additional dissection sessions are planned to further refine the guide and assess reproducibility with a larger cohort.

Conclusions: This study demonstrates the feasibility of adapting previously published ALL dissection techniques for use in preserved cadavers and integrating them into a first-year medical anatomy curriculum. Preliminary results suggest that the ALL can be reliably identified with proper technique, although novice learners may require more structured guidance and visual support. Future work will expand on these findings through increased data collection of identification of success rates as well as feedback on perceived difficulty of dissection procedures from student participants and anatomy facilitators.

HOLE ANATOMY WITH DISSECTION FROM NON-DRY SKULL FORMALIN FIXED, FRESH FROZEN AND GAX-SPECIMENS

K. west[1,2], J.D. Yankee[2], B. Benninger[1,2].

[1]Western University of Health Sciences, Lebanon, Oregon, UNITED STATES|

[2]Medical Anatomy Center, Western University of Health Sciences College of Osteopathic Medicine of the Pacific-Northwest, Lebanon, Oregon, UNITED STATES|

ABSTRACT BODY:

Purpose of Study: Craniotomy (Burr hole-BH) creates an opening in skull bone (frontal, parietal temporal, occipital bones) described supratentorial (anterior, middle fossa) or infratentorial (posterior fossa). Extra-axial hemorrhage (EXH) occurs within the skull outside of brain parenchyma. EXH's include epidural and subdural hematomas (EDH, SDH) resulting in traumatic brain injuries (TBI) requiring emergency department (ED) action. Delayed action (>70 mins) could worsen hematoma, causing increased intracranial pressure (ICP). EDH often results from middle meningeal artery (MMA) damage. EDH account for 10% of TBI with 7% to 30% mortality. SDH results in blood between dura and arachnoid mater. TBI may cause SDH/EDH with severe TBI and acute SDH ranging from 12% and 29%. Emergent BH criteria for SDH/EDH are identical. Indications for urgent BH in ED include expanding EDH with CT midline shift, deteriorating mental status with anisocoria, Glasgow Coma Scale< 8, and neurosurgery not available within 2 hours od insult. SDH, another life-threatening bleed resulting in blood between dura and arachnoid mater. Quick decision-making results in successful BH decompression. Study objective is to develop palpable and/or identifying landmarks standardizing supra/infra tentorial BH approaches on formalin fixed deceased-donors (FFxDD), fresh-frozen deceased-donors (FrFzDD) and GAXspecimens.

Methods Used: METHODS. Literature search was conducted on BH studies with FFxDD, FrFzDD and GAX-specimens. FFxDD n=42 (31M-11F)-84 total sides, FrFzDD n=16 (10M-6F)-32 total sides, GAX-specimen n=8(5M-3F)-8-sides underwent 2 supratentorial and 1 infratentorial BH sites: 1.)Frontal 10cm superior to midline neutral pupil, 2.)Temporal 2cm anterior x 4cm superior to external auditory meatus, and 3.)Occipital 1/3 distance between mastoid process and external occipital protuberance.

Summary of Results: RESULTS. Literature search revealed no known studies FFxDD, FrFzDD and GAX-specimens receiving non-CT BH. No vascular sinus damage noted FFxDD 1-Frontal 82/82; FrFzDD 32/32; and GAX-specimens 16/16. MMA site, 2- Temporal 78/82-95%; FrFzDD 30/32-94%; and GAX-specimens 15/16-94%. No vascular sinus damage 3-Occipital 77/82-94%; FrFzDD 29/32-91%; and GAXspecimens 15/16-94%.

Conclusions: This study was the first to compare FFxDD vs FrFzDD and GAX-specimens regarding palpable and/or visual landmarks for non- CT emergency BH to evacuate EDH/SDH. All 3 locations suggested low probability of damaging a vascular sinus while placing a BH near common EXH's.

GENICULATE GANGLION IDENTIFICATION VIA SKULL CAP DISSECTION: AN ANATOMIC GUIDE

B.H. Fardanesh, S. Melanahalli, C. Llera Martín.
Western University of Health Sciences College of Osteopathic Medicine of the Pacific, Pomona, California, UNITED STATES|

ABSTRACT BODY:

Purpose of Study: The geniculate ganglion is critical to Cranial Nerve VII (CN VII) function and is implicated in geniculate neuralgia, facial palsy, and herpes zoster oticus. Previous dissection typically requires removing parts of the cranial fossa or temporal bone, but these methods often damage the ganglion and lack reproducibility. This protocol offers structured guidance for skull cap dissection of the geniculate ganglion, emphasizing landmarks and technique for use in medical education and surgical training.

Methods Used: Skull cap dissections were performed on 8 adult donors from the Western University of Health Sciences Body Donation Program. The procedure involved a transverse cut of the skull from glabella to occiput base, followed by brain removal to expose the cranial fossa. The middle cranial fossa was accessed by locating the petrous ridge, and the dura overlying the middle fossa was reflected laterally to medially. The internal acoustic meatus served as a landmark for tracing CN VII, with the superior border aligned parallel to the sella turcica and the lateral border at the lateral rectus muscle. Bone was separated with a point and 0.5 cm chisel and mallet while maintaining a superficial plane to preserve nerves. As nerve structures become visible, the characteristic “knee-bend” configuration of the geniculate ganglion was identified, along with further tracing of both the greater petrosal and CN VII. This process concluded by identifying the inner ear ossicles, particularly the malleus and incus, lateral to the exposed ganglion.

Summary of Results: In 8 out of the 8 cadavers, the geniculate ganglion, CN VII main branch, the greater petrosal nerve, and all ear ossicles were consistently visualized with 7 of those cadavers preserving the ganglion in situ. This technique offered the additional benefit of revealing other relevant structures in the middle ear, expanding the anatomical insight gained during each dissection.

Conclusions: The described skull cap dissection protocol enabled reliable and clear exposure of the geniculate ganglion, facilitating identification through its distinct “knee-bend” appearance. The approach consistently provided excellent visualization of key neural elements, allowing differentiation between the geniculate ganglion, the CN VII, and the greater petrosal nerve. Systematic protocols for skull cap demonstrated strong reproducibility across multiple cadavers. Future work will assess the reproducibility of this guide and its dissections among medical student cohorts.

ASSESSING SHOULDER COMPRESSOR CUFF ROTATOR CABLE ANATOMY BETWEEN GAXSPECIMEN VS CONVENTIONAL FORMALIN PREPARED DECEASED-DONORS IMPROVING ANATOMICAL KNOWLEDGE

J. Yankee[1], E.M. Fulsher[1,2], R. hess[1,3], B. Benninger[2,3]

[1]Medical Anatomy Center, Western University of Health Sciences College of Osteopathic Medicine of the Pacific-Northwest, Lebanon, Oregon, UNITED STATES|

[2]Western University of Health Sciences, Lebanon, Oregon, UNITED STATES|

[3]Medical Anatomy Center, Western University of Health Sciences, Lebanon, Oregon, UNITED STATES|

ABSTRACT BODY:

Purpose of Study: The rotator cable (RCa), an important protective component of the rotator crescent of the compressor cuff (CCuff). RCa dominant fibres arise collectively from supraspinatus, infraspinatus and teres minor. RCa is a prominent reenforced band of fibrous tissue commonly identified on the articular surface of CCuff. Its function is thought to disperse energy across the humeral head protecting the CCuff from injury and enabling the comprehensive function allowed the glenohumeral joint. Recognized by MRI and ultrasound imaging as well as arthroscopy. Learning its anatomical variations is essential for diagnosing and managing CCuff injuries, especially in populations (>60yrs) where degenerative changes are common. Study objective is to develop standardized dissection approach to visualize RCa on GAXspecimen and formalin-fixed deceased-donors(FFDD).

Methods Used: Literature search was conducted to evaluate dissection techniques of RCa. GAX-specimen (n=14- sides:4-Males,8-sides:3-Females,6-sides), FFDD (n-28sides:10-Males:4-Females) underwent a modified dissection protocol designed by Benninger termed the delto-sono-crescent-cable dissection method, exposing RCa by reflecting deltoid and performing acromion osteotomy.

Summary of Results: Literature search revealed no known studies of GAX-specimen versus FFDD dissecting RCa. 38/42 shoulders exhibited an intact RCa, with an average thickness of 1.3 ± 0.6 mm and length of 11.7mm ± 1.3 mm. Findings suggest medical students can dissect the RCa and witness its integrity and contribution to degenerative CCuff changes. Benninger's delto-sono-crescent-cable method provides an effective means of visualizing RCa and other CCuff structures, offering insights into the varied functional roles and pathologies.

Conclusions: This study introduces a dissection technique reflecting the deltoid and conducting an acromion osteotomy demonstrating the RCa, an important aspect of the CCuff. Learning the anatomical, radiological and surgical details of the RCa and associated CCuff complex early in a health providers career will improve the acumen for identifying subtle pathologies, improving rehabilitation and successful surgery as part of successful treatment regimes.

BODYWORLDS HAND DISSECTION FOR MEDICAL TEACHING, TRAINING AND PATIENT DEMONSTRATION OF PATHOLOGY.

E.M. Fulsher, B. Benninger

Medical Anatomy Center, Western University of Health Sciences College of Osteopathic Medicine of the Pacific-Northwest, Lebanon, Oregon, UNITED STATES|

ABSTRACT BODY:

Purpose of Study: Hand can be placed in multiple planes shaped to accommodate extraordinary tasks including a powerful healing tool. Possesses 3 bony and muscle regions and 3 locations for nerves/artery entrance. Flexor/extensor pulley systems connected via unique muscles. Understanding the structural design is crucial for diagnosing, treating, rehabilitation, and prevention. Study objective was to dissect hands following BodyWorlds protocol revealing layers and structural ratios.

Methods Used: Dissect subcutaneous, layer-by-layer exposing major and nuanced structures preserving sensory nerves, vessels, ligaments, tendons, muscles, aponeuroses, and retinacula optimized for plastination and 3D teaching. Emphasizing radial/ulnar dorsal branches, median palmar distribution, palmar ulnar/median anastomoses, and arterial maps (radial/ulnar systems, arches, digital branches).

Summary of Results: Special preservation led to superficial branch radial nerve (SBRN), dorsal cutaneous branch ulnar nerve(DCBUN) ~5–8cm proximal to wrist, palmar cutaneous branch of median nerve(PCBMN) ~4–6cm proximal to wrist (outside tunnel), palmar cutaneous branch of ulnar nerve(PCBUN) ~3–5cm proximal to wrist, palmar aponeurosis–palmaris complex with palmaris brevis were dissected. Volar fascia and flexor retinaculum complex featured in 2 planes. Guyon's canal (GC) superficial to transverse carpal ligament (TCL) with pisiform(medial), hook of hamate(lateral), TCL/hypothenar fascia as floor. Zones documented:Zone 1 (pre bifurcation, mixed), Zone 2 (deep motor), Zone 3 (superficial sensory). Dorsal/extensor retinaculum preserved maintaining extensor compartment topology and fortitude. Osseofibrous anchorage points preserved, dorsolateral distal radius (proximal to radial styloid) and dorsomedial distal ulna (proximal to ulnar styloid). Digital sheath exposed (digits 3,4), fibrous digital sheath/vaginalis fascia (select pulley windows) exposing Camper's chiasm, FDS splits on the proximal phalanx, FDP passes through split to distal phalanx, explicitly revealed on 3rd and 4th digits. Ultrasound (US) guided layer recognition (pre/peri dissection planning) of volar wrist. US & doppler localizes ulnar and radial arteries, cross-sectional median nerve at tunnel oriented to GC and superficial to TCL before opening surgical plane, reducing iatrogenic injury to small branches.

Conclusions: BodyWorlds dissection protocol, vascular contrast and plastination reveals clinically important landmarks of various hand regions for education.

IDENTIFYING THE HOFFA (INFRAPATELLAR) FAT PAD WITH INFRAPATELLAR PLICAE (LIGAMETUM MUCOSUM) FROM CADAVER POCUS ULTRASOUND AND DISSECTION OF THE KNEE JOINT WILL PROVIDE A MENTAL TEMPLATE OF ITS MORPHOLOGY AND ASSOCIATED PATHOLOGIES.

J.L. Mccluskey[1], L. Arsenault[1], B. Benninger[2].

[1]Medical Anatomy center, Western University of Health Sciences, Pomona, California, UNITED STATES|

[2]Medical Anatomy Center, Western University of Health Sciences College of Osteopathic Medicine of the Pacific-Northwest, Lebanon, Oregon, UNITED STATES|

ABSTRACT BODY:

Purpose of Study: Knee joint pathology is extremely common and debilitating. The knee has a known structure of fat named 'Hoffa's fat pad which has a characteristic shape and has been found to be associated with pain and knee deterioration which can result in osteoarthritis. Hoffa's knee disease/syndrome is a common condition and is a severe pathology of the knee joint in many subjects. POCUS ultrasound can be a convenient method of primary diagnosis of this pathology. However, in the literature only a single study provided an analysis of the characteristic ultrasound image of Hoffa's disease/syndrome regarding its most common and pathognomonic symptoms. The study objective was to identify Hoffa's fat pad with POCUS ultrasound and cross-sectional scanning comparing cadaver preparations with subsequent dissection of the fat pad assessing its morphology.

Methods Used: Literature search revealed no known cadaver studies regarding ultrasound and cross-sectional imaging of knee fat pad and associated structures. Exclusion criteria included knee replacement and/or multiple knee surgeries. Novel GAX prepared cadavers (n=12 knees from six bodies, M=4, F=2) and traditional embalmed cadavers-TEC (n=26 knees from 15 bodies, M=9, F=6) were scanned with MRI, CT and handheld GE Vscan Air probes, followed by open dissection. Four knees from TEC were excluded for a total of 38 knees.

Summary of Results: POCUS ultrasound identification of the fat pad was confirmed on all knees with the TEC knees having a broader range of poor image quality. 12 GAX knees had supeior quality image acquisition versus the 38 TEC knees. GAX dissection revealed lifelike dermis during knee palpation and range of motion, knee fat pads and associated structures were realistic regarding texture, responsiveness to surgical tools, hydration and appearance. The TEC knees had a hardened waxy dermis, essentially no range of motion which made palpation very difficult, fat pads and associated structures were very firm and less compliant, decrease responsiveness to surgical tools, dehydrated and dull in color fat pad.

Conclusions: Based on the two types of cadaver embalming, imaging and dissection included in this study, GAX prepared bodies versus TEC demonstrated superior POCUS identification and dissection of Hoffa's fat pad suggesting a fertile training medium integrating ultrasound with dissection.